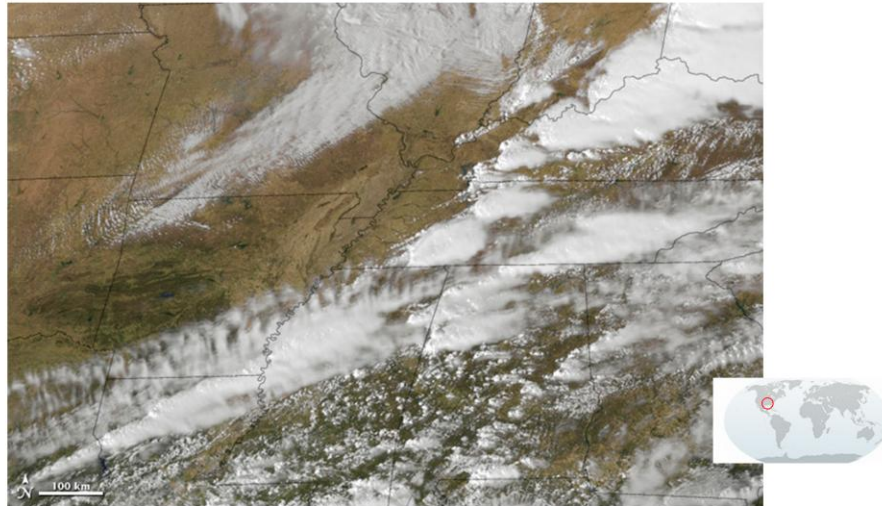


Tornadoes Sweep across Midwest and Appalachians March 2, 2012



Tornadoes cause an average of 70 fatalities and 1,500 injuries in the U.S. each year. ~40 fatalities in this weeks tornadoes.

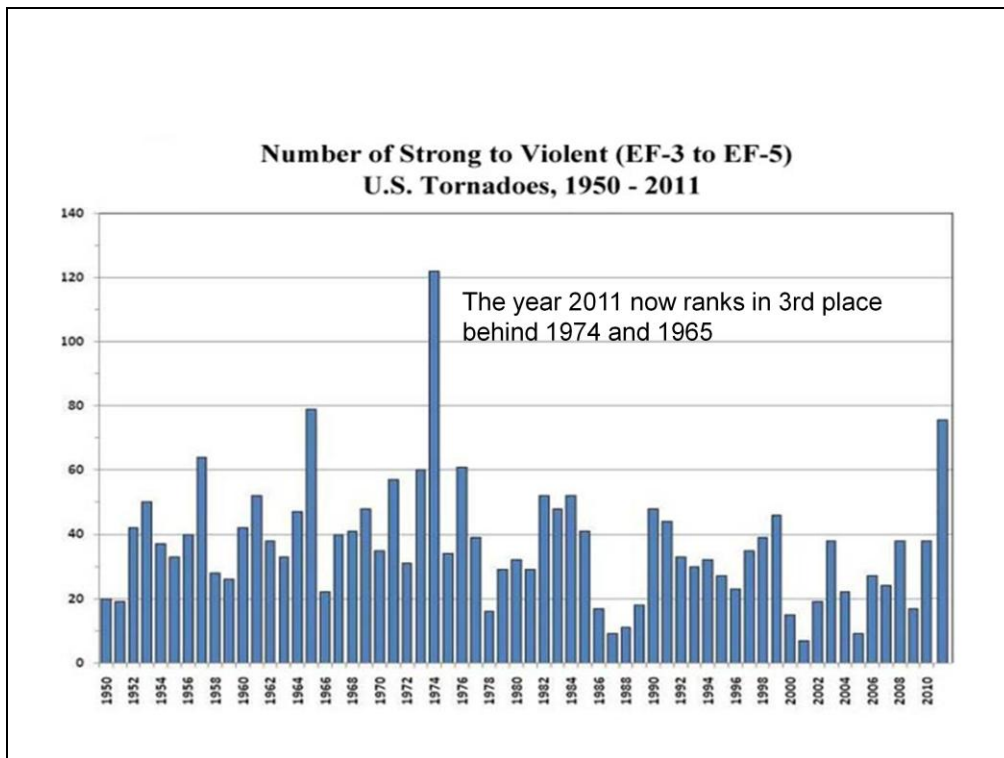
Severe thunderstorms and tornadoes swept across the Midwest and Appalachians on March 2, 2012. According to CNN, at least [36 people were killed](#), with the majority of the victims in Indiana and Kentucky. On the Weather Underground blog, meteorologist Jeff Masters [described the outbreak](#) as a result of warm, wet air from the Gulf of Mexico mixing with cold, dry air aloft.

This animation is a combination of thermal infrared (heat) and visible imagery from the [Geostationary Operational Environmental Satellite-East \(GOES-East\)](#), and a [color map](#) from the [Moderate Resolution Imaging Spectroradiometer \(MODIS\)](#). The animation begins at 12:01 a.m. EST (0501 UTC) March 2 , and continues until 12:01 EST (0501 UTC) March 3.

References

CNN. (2012, March 3). [Rescuers scour for survivors after string of killer storms](#). Accessed March 3, 2012.

Masters, Jeff. (2012, March 3). [High risk of a major tornado outbreak today; 13 dead from Leap Day outbreak](#). Accessed March 3, 2012.

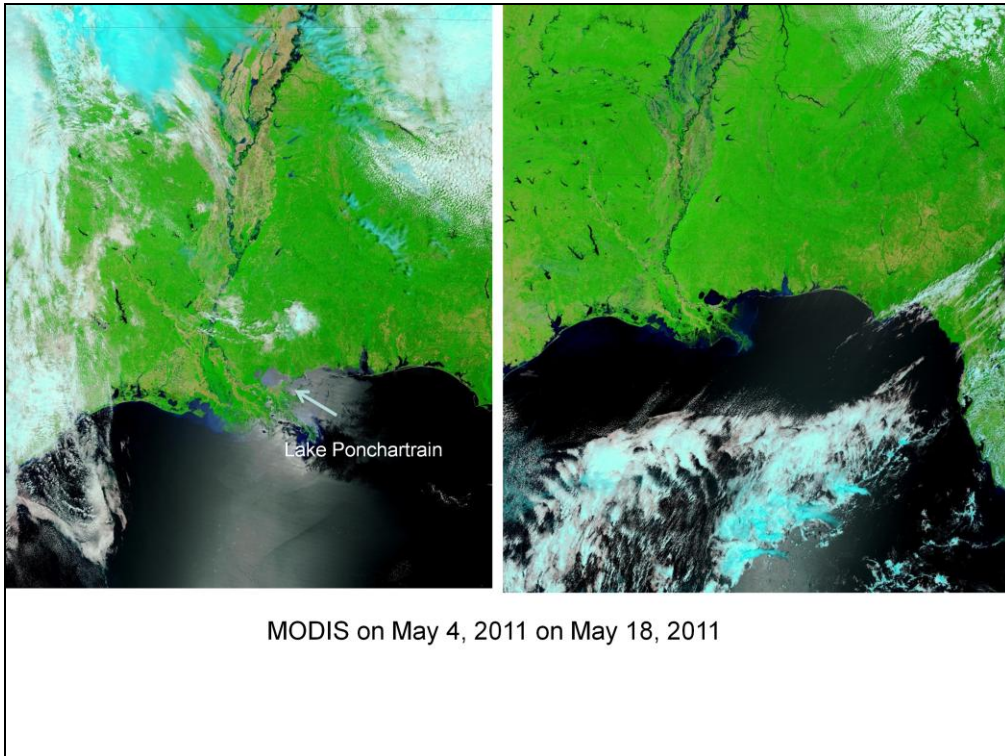


The year 2011 will forever be known as Year of the Tornado in the U.S. A series of violent severe storms swept across the Plains and Southeast U.S., bringing an astonishing six billion-dollar disasters in a three-month period. The epic tornado onslaught killed 552 people and caused \$25 billion in damage. Three of the five largest tornado outbreaks on record hit in a six-week period, including the largest and most expensive tornado outbreak in U.S. history—the \$10.2 billion dollar Southeast U.S. Super Outbreak, April 25 – 28. Even more stunning was the \$9 billion late-May tornado outbreak that brought an EF-5 tornado to Joplin, Missouri. The Joplin tornado did \$3 billion in damage and killed 158 people—the largest death toll from a U.S. tornado since 1947, seventh deadliest tornado in U.S. history, and the most expensive tornado in world history. In a year of amazing weather extremes, this year’s tornado season ranks as the top U.S. weather story of 2011.



Clouds were banked against the California coastline and skies were filled with smoke on July 13, 2008, when the Moderate Resolution Imaging Spectroradiometer (MODIS) on NASA's Terra satellite captured this image of the state. Forest fires have been burning in the area since the first week of summer, when thousands of lightning strikes occurred during a weekend of "dry" thunderstorms. Places where MODIS detected active fire are outlined in red.

The high-resolution image provided above is at MODIS' maximum spatial resolution (level of detail) of 250 meters per pixel, and it shows the entire state of California. The MODIS Rapid Response Team provides twice-daily images of Northern and Southern California in additional resolutions and formats, including an infrared-enhanced version that highlights burned ground. NASA image courtesy the MODIS Rapid Response Team. Caption by Rebecca Lindsey



MODIS acquired the left image on May 4, 2011, and the right image on May 18, 2011. Both images use a combination of visible and infrared light to increase contrast between water and land. Water ranges in color from gray-blue to navy. (Lake Pontchartrain appears silvery blue on May 18 due largely to the angle of sunlight.) Vegetation is green. Bare ground is brown. Clouds are pale blue-green and cast shadows.

Both images show flooded conditions along the Mississippi River. A significant difference between the images, however, is the water visible in the Morganza Floodway on May 18. The Army Corps of Engineers reported that the discharge in the floodway was 108,000 cubic feet per second on May 18, the floodway's fifth day of operation in 2011.

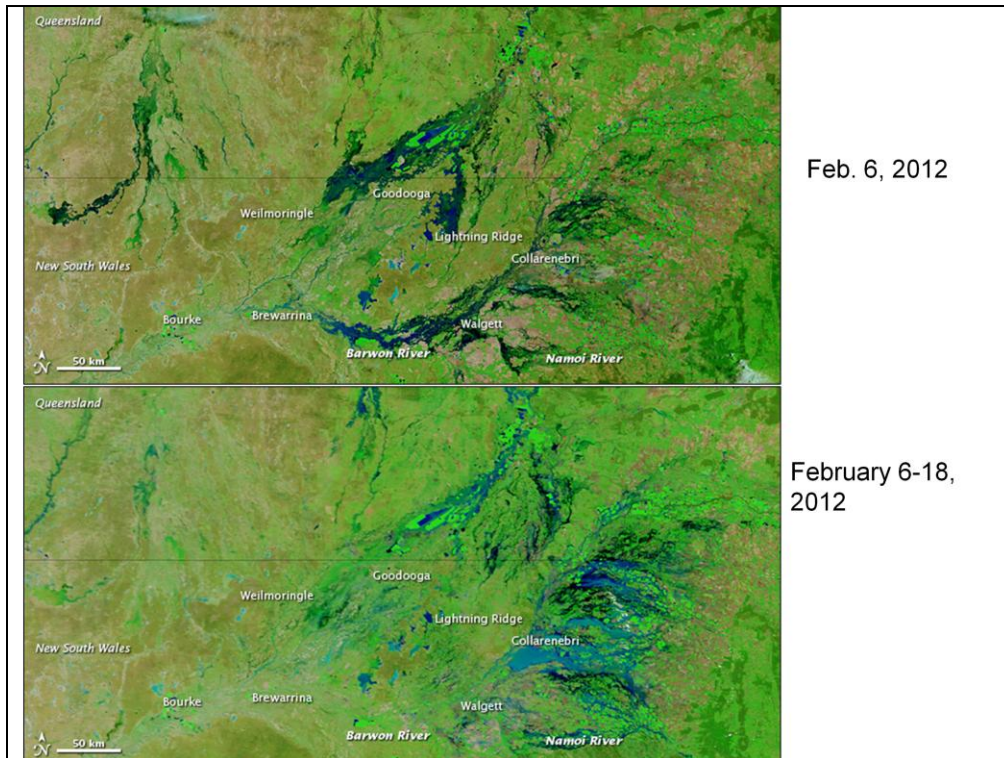


Mississippi River spilled over its banks in Arkansas and Tennessee on May 12, 2011



Photo from Space Station

The Mississippi River spilled over its banks in Arkansas and [Tennessee](#) on May 12, 2011, as the International Space Station passed overhead. This astronaut photograph shows muddy water sitting on floodplains around Tomato, Arkansas, as well as extensive flooding to the north. Flood waters around Tomato appear confined by an embankment in the west. The embankment extends southward from a bend in the Mississippi. West of the embankment lies a patchwork of agricultural fields. East of the river lies an expanse of dark green forest, the Anderson-Tully State Wildlife [Management](#) Area.



Along the border between the Australian states of Queensland and New South Wales, several communities were flooded in early February 2012. By mid-month, the flood waters had moved west. On February 19, online news source NineMSN reported that as many as 10,000 residents of northeastern New South Wales would likely be isolated from the outside world by high water.

The Moderate Resolution Imaging Spectroradiometer ([MODIS](#)) on NASA's [Terra](#) satellite acquired these images on February 18, 2012 (top), and February 6, 2012 (bottom). Both images show flood conditions, but they also show the movement of water along the Barwon and Namoi Rivers and other waterways in the region.

These images use a combination of visible and infrared light to better distinguish between water and land. Water varies from electric blue to navy, with darker shades generally indicating deeper water. Vegetation is bright green. Bare ground is earth-toned.

On February 6, floods are largely confined to areas east of Walgett. By February 18, flooding has receded east of that town, but floods have traveled westward along tributaries of the Darling River. New flooding is especially apparent between Walgett and Brewarrina, and north of Lightning Ridge and Goodooga.

NineMSN reported that several thousand residents were already isolated in the communities of Walgett, Collarenebri, Weilmoringle, and Goodooga, and flooding in those areas could persist for weeks. Floods were also expected in Brewarrina and

Bourke over the next month.

References

NineMSN. (2012, February 19). [Warnings issued as NSW floods creep west](#). Accessed February 20, 2012.

NASA images courtesy [LANCE/EOSDIS MODIS Rapid Response Team](#) at NASA GSFC. Caption by Michon Scott.

Instrument: Terra - MODIS

Iceland's Grimsvotn Volcano began erupting on May 21, 2011

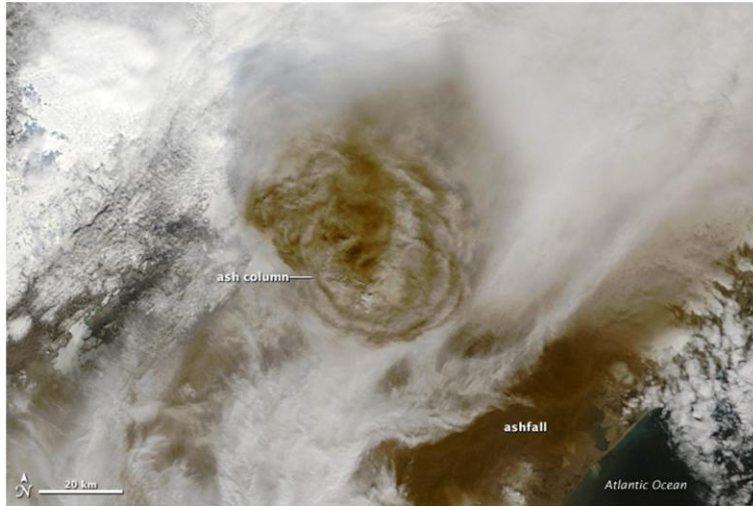


Image May 22, 2011 MODIS

About 14 months after [Eyjafjallajökull rumbled to life](#), another volcano on Iceland began spewing ash and steam. At approximately 17:30 UTC (5:30 p.m. local time) on May 21, 2011, Grimsvötn began to erupt, the Icelandic Met Office reported. The volcano sent a plume of volcanic ash and steam about 20 kilometers (12 miles) above sea level. Overnight, the plume height dropped to 15 kilometers (9 miles), but occasionally re-approached its initial altitude.

The Moderate Resolution Imaging Spectroradiometer ([MODIS](#)) on NASA's [Terra](#) satellite captured this natural-color image at 13:00 UTC (1:00 p.m. local time) on May 22, 2011. (MODIS on NASA's [Aqua](#) satellite captured [another image](#) of the volcano a 8 hours earlier.)

Above Grimsvötn's summit, volcanic ash forms a roughly circular plume that towers above the surrounding clouds. In the southeast, ash has colored the snow surface dark brown. Ash from the volcano reduced visibility to about 50 meters (160 feet) in some places, the Eruptions blog stated. Iceland Review Online reported that ash falling from the volcano caused some areas turn as dark as night in the middle of the day. The ash plume also prompted the closure of Keflavik, Iceland's largest airport.

The initial plume from Grimsvötn was higher than that from Eyjafjallajökull, which only reached 8 kilometers (5 miles). Despite its taller plume, Grimsvötn was expected to hamper trans-Atlantic air traffic less than Eyjafjallajökull had, at least in the first 24 hours. Grimsvötn's ash was forecast to travel toward the northeast, the Icelandic Met Office stated. In addition, the ash content was coarser and therefore less likely to remain airborne long enough to reach European airspace. Some volcanic ash models, however, suggested that Grimsvötn's ash could interfere with flights in the United Kingdom and Ireland beginning on May 24.

Volcanic plumes can produce lightning, and the plume from Grimsvötn produced an [intense lightning storm](#). At its peak, the lightning storm from this volcano produced 1,000 times as many lightning strikes per hour as [Eyjafjallajökull had](#) over a year earlier.

Much of Grimsvötn lies below the [Vatnajökull Glacier](#). Consequently, when the volcano first started erupting in May 2011, the eruption was subglacial. Such eruptions can cause glacier outburst floods, or jökulhlaups. The Icelandic Met Office stated, however, that because an outburst flood had already occurred the previous autumn, a big flood appeared unlikely in the spring of 2011.

References

Global Volcanism Program. (n.d.) [Grimsvötn](#). Accessed May 23, 2011.

Iceland Review Online. (2011, May 22). [Ash from Grimsvötn Volcano visible around Iceland](#). Accessed May 23, 2011.

Icelandic Met Office. (2011, May 21). [Eruption has started in Grimsvötn](#). Accessed May 23, 2011.

Icelandic Met Office. (2011, May 22). [Ash plume and lightning](#). Accessed May 23, 2011.

Klemetti, E. (2011, May 21). [Subglacial eruption starting at Iceland's Grimsvötn](#). Eruptions. Accessed May 23, 2011.

Klemetti, E. (2011, May 21). [More information on the May 21 eruption of Grimsvötn in Iceland](#). Eruptions. Accessed May 23, 2011.

Klemetti, E. (2011, May 22). [Grimsvötn eruption closes Keflavik Airport near Reykjavik \(and more images of the eruption\)](#). Eruptions. Accessed May 23, 2011.

Klemetti, E. (2011, May 22). [Keeping tabs on the Grimsvötn eruption as the ash spreads towards Europe](#). Eruptions. Accessed May 23, 2011.

News Blog. (2011, May 23). [In 2011, Grimsvötn is the new Eyjafjallajökull](#). *Nature*. Accessed May 23, 2011.

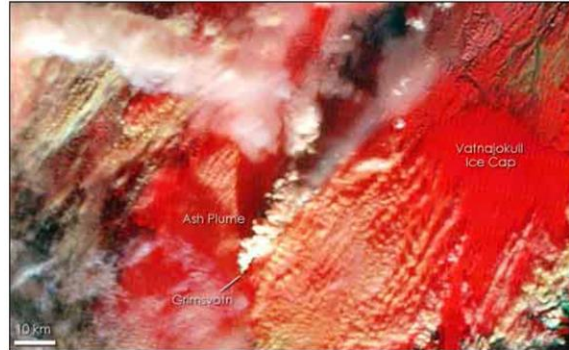
NASA image courtesy Jeff Schmaltz, [MODIS Rapid Response Team](#) at NASA GSFC. Caption by Michon Scott and Robert Simmon.

Instrument: Terra - MODIS

Iceland's Grimsvotn Volcano began erupting on November 2, 2004



Natural Color (red=670 nm, green=565 nm, blue=479 nm)



False Color (red=479 nm, green=1,652 nm, blue=2,155 nm)

Iceland's Grimsvotn Volcano began erupting on November 2, 2004, forcing officials to divert air traffic from the region to prevent ash from damaging aircraft engines. The volcano sits beneath the Vatnajokull Ice Cap, Europe's largest glacier, and is Iceland's most frequently active volcano. This eruption may be connected to the draining of a glacier lake in the volcano's caldera. Buried under a 200-meter thick ice shelf, the lake is under extreme pressure. Melting water fills the lake, and when levels are high enough, the water lifts the ice dam, draining the lake. Grimsvotn Lake drained in mid-October, lifting some of the pressure from the volcano. The flood was followed by a series of earthquakes, and on November 2, an eruption. As of November 3, the eruption was still occurring, and ash was reported to have drifted as far northeast as Finland.

The Moderate Resolution Imaging Spectroradiometer ([MODIS](#)) on NASA's [Terra](#) satellite captured this view of the erupting volcano. The plume is largely made of steam rising from the melting ice above the volcano, but ash is mixed in as well. Against the white of the Vatnajokull Ice Cap, the white eruption plume is difficult to see in the true color image. The false color image, which shows ice as bright red, provides the contrast needed to see the steam plume. As the plume is blown north, the steam dissipates, and the dark ash is more visible. The shadow on the snow along the top edge of the image may be ash on the glacier.

As the eruption continues, flooding is likely around the volcano. So far, some of the glacier-fed rivers southeast of the volcano have flooded, and more floods are expected.

The high-resolution images provided above are at MODIS's maximum resolution of 250 meters per pixel. The MODIS Rapid Response Team provides both the [true](#) and [false](#) color images in additional resolutions.

NASA images courtesy Jacques Desclotres, [MODIS Rapid Response Team](#) at NASA GSFC

Instrument: Terra - MODIS



The MODIS instrument on NASA's Aqua satellite captured a false-color image (top) of the ash plume on May 16, 2010. The volcanic plume is yellow, while clouds are various shades of white to light gray. Darkest areas are cloud-free views of the ocean. The bottom image is from the CALIPSO satellite and is a vertical profile of the atmosphere, revealing that the ash was between four and six kilometers (2.5-3.5 miles) high on May 16. Credit: NASA Goddard MODIS Rapid Response Team, Jesse Allen/NASA CALIPSO Project, Chip Trepte

Many satellites can provide a bird's-eye view that can identify thick plumes of ash, but few satellites can tell how high the ash is in the atmosphere. The Cloud-Aerosol Lidar and Infrared Pathfinder Satellite Observations (CALIPSO) satellite, however, records a vertical profile of the atmosphere, which reveals the altitude of ash clouds. These observations help modelers in volcanic ash advisory centers improve forecasting models and issue more accurate warnings to pilots and others with aviation interests.

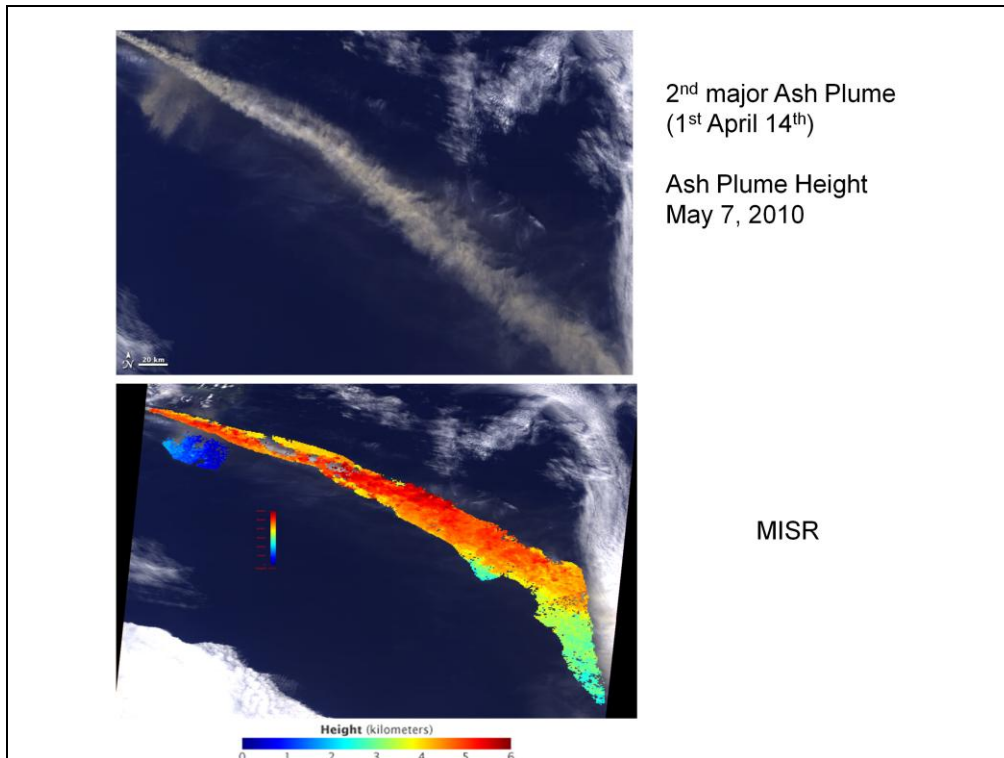
The Moderate Resolution Imaging Spectroradiometer (MODIS) on NASA's Aqua satellite captured a night-time image of the Eyjafjallajökull Volcano's ash plume on May 16, 2010. The image showed subtle differences in thermal energy radiated by volcanic emissions, the open ocean, and water and ice clouds. The MODIS image revealed the plume extended from the Eyjafjallajökull Volcano in Iceland to the U.K.

The CALIPSO Satellite image showed a vertical profile of the atmosphere, revealing that the ash was between four and six kilometers (~3.5 miles) high on May 16. A joint mission between NASA and the French Centre National d'Etudes Spatiales (CNES), CALIPSO carries a pulsating laser (lidar) that sends short pulses of light through the atmosphere. Some of the light bounces off clouds and particles in the atmosphere and returns to the satellite. The strength of the returning signal provides information about the characteristics of the clouds or particles.

The length of time CALIPSO's lidar's light pulse takes to return to the satellite provides information about where the clouds or particles are in the atmosphere. On May 16, a bank of clouds covered much of the ocean at an altitude of about two kilometers. Breaks in the clouds are represented by a drop in altitude in the atmospheric profile—showing how the laser light being scattered back to the satellite was coming from farther away. In the north, the cloud cover is less uniform, with scattered clouds creating jagged peaks in the profile. The volcanic ash is above the clouds at about six kilometers high, the altitude at which models predicted it would be.

The London Volcanic Ash Advisory Center at the UK Met Office uses satellite measurements like these to validate model results. The models integrate weather forecasting models with models of the way ash moves through the atmosphere to predict where volcanic ash will be. The satellite measurements give modelers a way to check their predictions and improve future forecasts. NASA Langley Research Center produces expedited CALIPSO data. Data and images compatible with Google Earth are available from the Goddard Earth Sciences Data and Information Services Center.

Text credit: Holli Riebeek/NASA's Earth Observatory/NASA Goddard Space Flight Center



Iceland's Eyjafjallajökull Volcano produced its second major ash plume of 2010 beginning on May 7. When the first ash eruption began on April 14, air travel across most of Europe was shut down, but by the time of the second eruption, forecasters were better prepared to predict the spread of volcanic ash. Despite some airport closures and flight cancellations, most air passengers completed their journeys with minimal delay.

Among the key pieces of information that a computer model must have to predict the spread of ash is when the eruption happened, how much ash was ejected, and how high the plume got. The [Multi-angle Imaging SpectroRadiometer](#) (MISR) aboard NASA's [Terra](#) satellite collected data on ash height when it passed just east of the Eyjafjallajökull Volcano mid-morning on May 7.

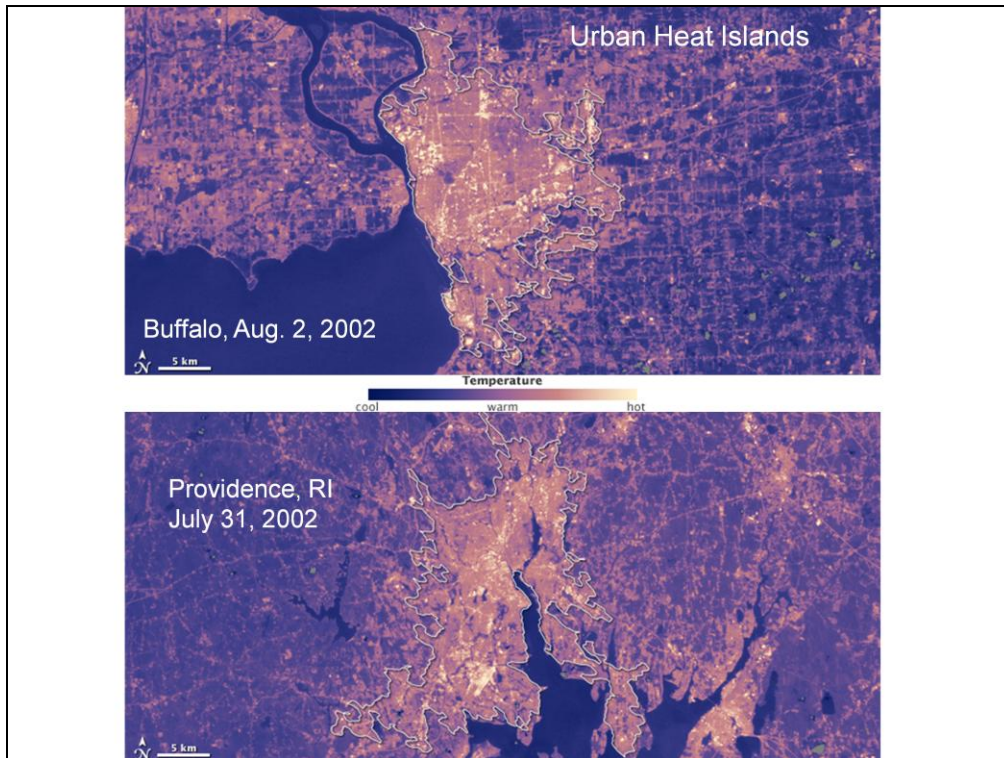
MISR has nine different cameras, each viewing the scene below from a difference angle nearly simultaneously. By combining all these images using a hyper-stereo technique, scientists can calculate the height of the ash plume.

The top image is a natural-color, nadir (downwards-looking) view of the scene, with the volcano itself just off the upper left corner of the image, and the main plume extending to the southeast. The bottom image is the stereo-derived plume height. Each pixel in the image shows an area 1.1 kilometers (0.68 miles) wide. The vertical accuracy is about half a kilometer (0.3 mile).

Much of the plume resides between 4 and 6 kilometers (2.5 and 4 miles) above the ocean surface (orange and red color in the right image), but the ash descends to near 3 kilometers (2 miles) (yellow-green) far downwind. Note also the smaller patch of ash, within about 1 kilometer (0.6 mile) of the surface (blue), which appears to be traveling to the southwest. This ash was on the ground and was then resuspended by low-level winds.

The Terra satellite is in a polar orbit, crossing the equator on the day side at about 10:30 a.m. With MISR's 400-kilometer-wide swath, it images the entire Earth about once per week, every two to four days at higher latitudes. Another instrument on Terra, the [Moderate Resolution Imaging Spectroradiometer](#) (MODIS), has a single viewing perspective, but a 2,300-km-wide swath, offering complementary, daily coverage of the volcanic plumes. The combination of MODIS area coverage and MISR plume height maps provides among the best constraints for ash plume modeling. These data are being used in continuing studies of the Eyjafjallajökull ash plume.

NASA image courtesy GSFC/LaRC/JPL MISR Team. Caption by Ralph Kahn and the MISR Team.



By evaporating water, plants cool their surroundings. By replacing plants with impervious surfaces, cities trap heat, and create a phenomenon known as the urban heat island. A variety of factors affect the urban heat island. Bigger cities tend to have stronger heat-trapping capacities than smaller cities. Cities surrounded by forest have more pronounced heat islands than do cities in arid environments. A new study, presented at the 2010 Fall Meeting of the American Geophysical Union, found that a city's layout—whether sprawling or compact—can also affect the potency of its urban heat island.

These images compare Buffalo, New York, on August 3, 2002 (top), and Providence, Rhode Island, on July 31, 2002 (bottom). Acquired by the Enhanced Thematic Mapper on NASA's Landsat 7 satellite, they show temperature, ranging from blue (warm) to yellow (hot). White lines delineate city limits.

Providence and Buffalo are roughly the same size, and both fall within the study area chosen by the research team: the forested environments in the northeastern United States. By choosing cities that are similar in size, and situated in similar environments, researchers can better compare city development patterns and their corresponding urban heat islands.

The researchers found that Providence has a denser development pattern than Buffalo, and a greater heat island effect. About 83 percent of Providence is densely developed, whereas just 46 percent of Buffalo is densely developed. Providence has surface temperatures roughly 12.2 degrees Celsius (almost 22 degrees Fahrenheit) warmer than its surroundings, whereas Buffalo has surface temperatures just 7.2 degrees Celsius (almost 13 degrees Fahrenheit) warmer than its surroundings.

Although the cities' development patterns differ, the nature of their surroundings also plays a role. Dense forest surrounds Providence while a mix of forest and farmland surrounds Buffalo. The urban heat island effect is more pronounced when forest rings a city.

Urban heat island research has significant implications for human health. In the middle of an already hot summer, the urban heat island effect can be deadly, especially at night. Round-the-clock heat means that city residents have no respite, and those who manage to sleep through the night may not drink enough water to stay hydrated. Although air conditioning provides relief, not everyone has access to it, especially poorer neighborhoods and developing nations. Where available, some kinds of air conditioning can raise outside temperatures.

Some measures can mitigate the urban heat island. Painting roads and rooftops white instead of black enables those surfaces to reflect more sunlight and absorb less heat. Planting vegetation on rooftops also reduces surface temperatures.

References

Imhoff, M.L. Zhang, P., Wolfe, R.E., Bounoua, L. (2010). [Remote sensing of the urban heat island effect across biomes in the continental USA](#). *Remote Sensing of Environment*, 114(3), 504–513.

Voiland, A. (2010, December 13). [Satellites pinpoint drivers of urban heat islands in the northeast](#). NASA. Accessed December 13, 2010.

Zhang, P., Imhoff, M.L. Wolfe, R.E., Bounoua, L. (2010). Detecting urban heat island drivers in northeast USA cities using MODIS and Landsat products. American Geophysical Union Fall 2010 Meeting.

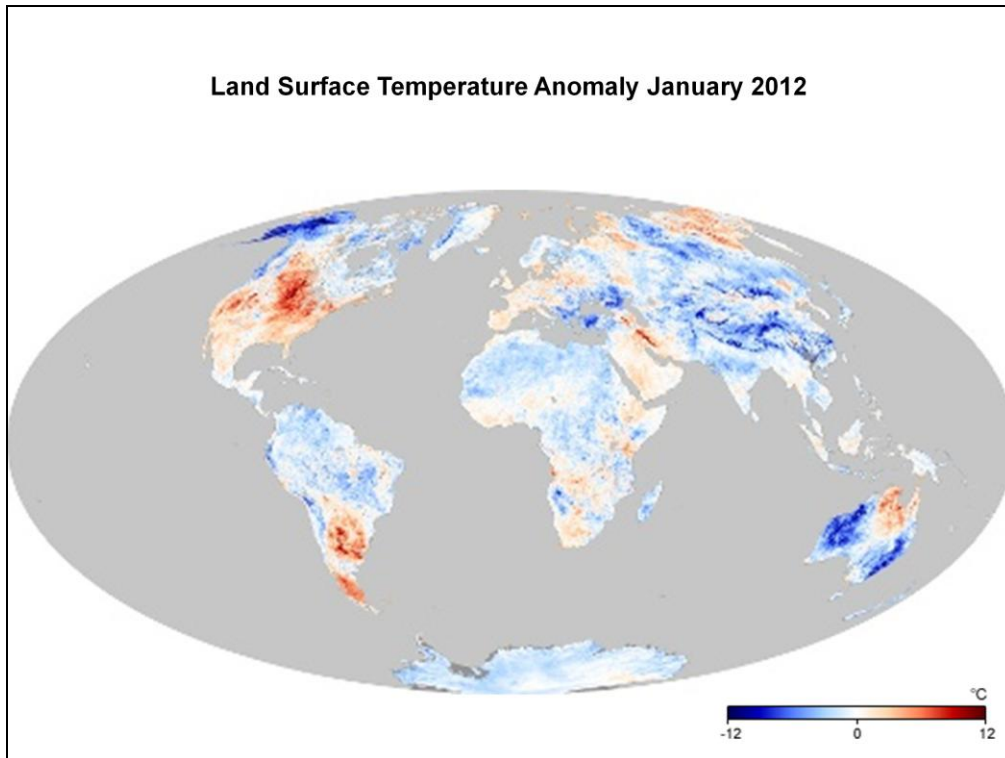
Links

[Beating the Heat in the World's Big Cities](#)

[Urban Heat Island: Baltimore, MD](#)

[New York City Temperature and Vegetation](#)

NASA Earth Observatory image created by Jesse Allen and Robert Simmon, using Landsat data provided by the [United States Geological Survey](#). Caption by Michon Scott.



Land surface temperature is how hot the “surface” of the Earth would feel to the touch in a particular location. From a satellite’s point of view, the “surface” is whatever it sees when it looks through the atmosphere to the ground. It could be snow and ice, the grass on a lawn, the roof of a building, or the treetops in a forest. Thus, land surface temperature is not the same as the air temperature that is included in the daily weather report.

An anomaly is when the conditions depart from average conditions for a particular place at a given time of year. The maps show daytime land surface temperature anomalies for a given month compared to the average conditions during that period between 2000-2008. Places that were warmer than average are red, places that were near normal are white, and places that were cooler than average are blue. The observations were collected by the Moderate Resolution Imaging Spectroradiometer ([MODIS](#)) on NASA’s [Terra](#) satellite.

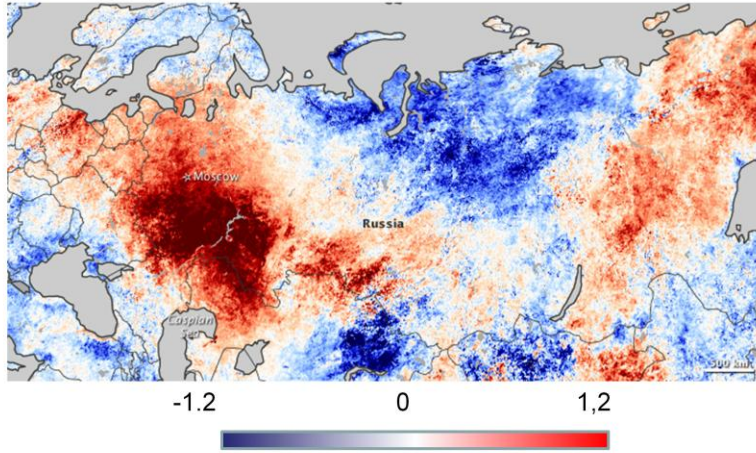
Some land surface temperature anomalies are simply random weather phenomena, not part of a specific pattern or trend. Others anomalies are more meaningful. Widespread cold anomalies may be an indication of a harsh winter with lots of snow on the ground. Small, patchy warm anomalies that appear in forests or other natural ecosystems may indicate deforestation or insect damage. Many urban areas also show up as hot spots in these maps because developed areas are often hotter in the daytime than surrounding natural ecosystems or farmland. Warm anomalies that persist over large parts of the globe for many years can be signs of global warming.

View, download, or analyze more of these data from NASA Earth Observations

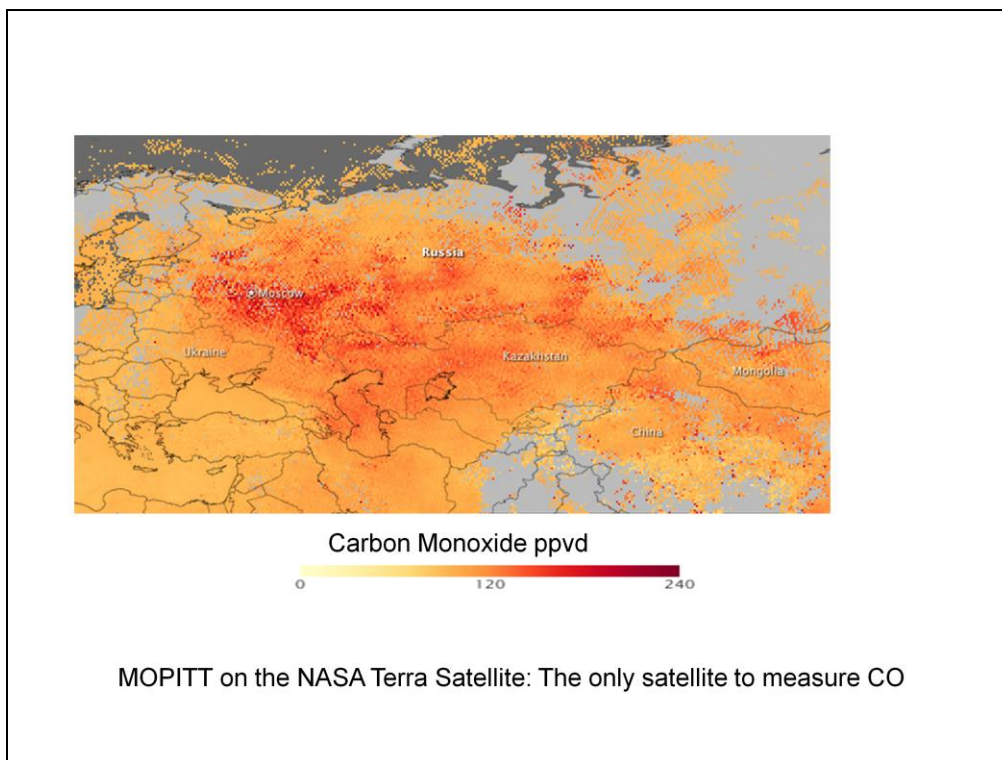
(NEO): [Land Surface Temperature Anomaly](#)

[download large image](#) (1 MB, JPEG)

Land Surface Temperature Anomaly (°C) Russia 2011



July 20-27, 2010



Even as Muscovites choked under a blanket of thick smoke in the first week of August 2010, concentrations of a colorless, odorless gas spiked to dangerous levels. A product of fire and a component of smoke, carbon monoxide is among the pollutants that wildfires spread across much of western Russia. This image, made with data from the Measurements of Pollution in the Troposphere ([MOPITT](#)) sensor flying on NASA's [Terra](#) satellite, shows carbon monoxide over western Russia between August 1 and August 8, 2010.

The highest levels of carbon monoxide are shown in red, while lower levels are yellow and orange. Western Russia, including Moscow, sits under a broad area of elevated carbon monoxide. Areas where the sensor did not collect data during the period—probably because of clouds—are gray.

MOPITT measures carbon monoxide in the atmosphere between two and eight kilometers above Earth's surface. The image shows the composite of those measurements, not carbon monoxide levels near the ground. However, ground measurements of carbon monoxide during the period reached more than six times higher than acceptable levels in Moscow, said news reports.

Carbon monoxide is a dangerous product of fire. The gas can remain in the atmosphere for weeks after being emitted and can therefore travel long distances from the fire that produced it. When it is near the ground where people can breathe it, carbon monoxide poses a health risk. Carbon monoxide binds to red blood cells more easily than oxygen, so it limits the amount of oxygen blood carries through the body. This causes a range of problems from headaches, nausea, and dizziness to cardiovascular problems and confusion. Carbon monoxide is also an ingredient in the production of ground-level ozone, which causes a number of respiratory problems.

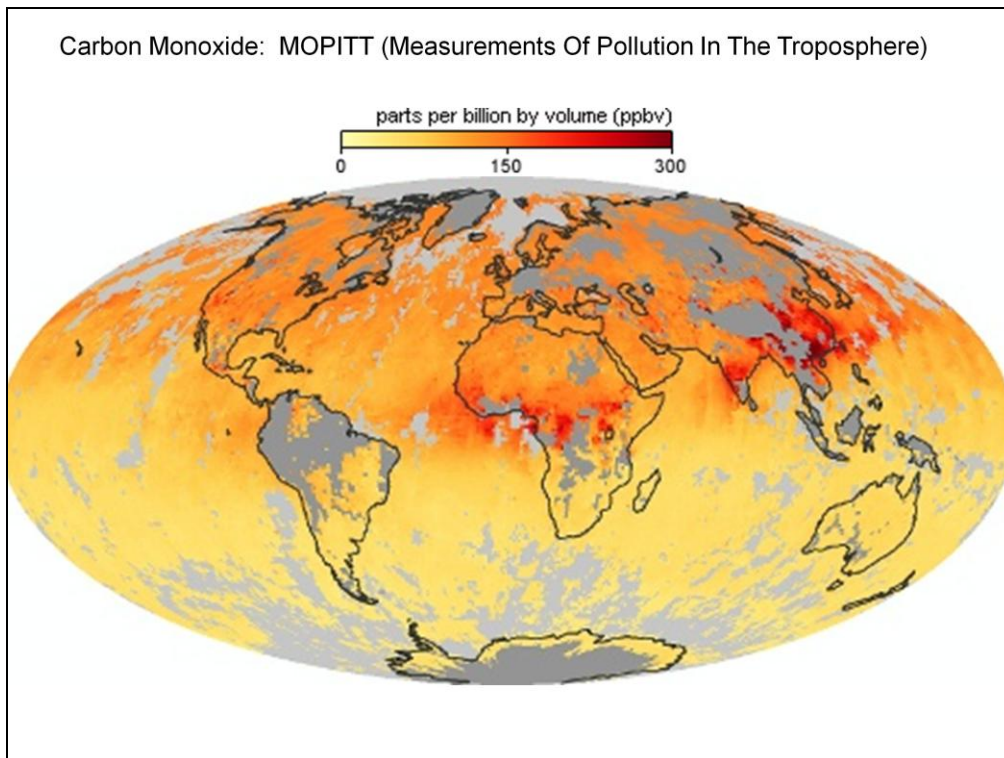
References

- Centers for Disease Control and Prevention. (2009, April 27). [Moscow smoke pollution delays flights as fires spread](#). Bloomberg Businessweek. Accessed August 9, 2010.
- United States Environmental Protection Agency. (2008, May 9). [Carbon Monoxide](#). Accessed August 9, 2010.
- United States Environmental Protection Agency. (2008, May 9). [Ground-level Ozone](#). Accessed August 9, 2010.

[More images of this event in Natural Hazards](#)

NASA Earth Observatory image created by Jesse Allen, using data provided by Gabriele Pfister, the National Center for Atmospheric Research (NCAR) and the University of Toronto [MOPITT Teams](#). Caption by Holli Riebeek.

Instrument: Terra - MOPITT



Colorless, odorless, and poisonous, carbon monoxide is one of the six major air pollutants regulated in the United States and in many other nations around the world. When carbon-based fuels, such as coal, wood, and oil, burn incompletely or inefficiently, they produce carbon monoxide. The gas is spread by winds and circulation patterns throughout the lower atmosphere (called the troposphere).

These maps show monthly averages of global concentrations of tropospheric carbon monoxide at an altitude of about 12,000 feet. The data were collected by the MOPITT (Measurements Of Pollution In The Troposphere) sensor on NASA's Terra satellite. Concentrations of carbon monoxide are expressed in parts per billion by volume (ppbv). A concentration of 1 ppbv means that for every billion molecules of gas in the measured volume, one of them is a carbon monoxide molecule. Yellow areas have little or no carbon monoxide, while progressively higher concentrations are shown in orange and red. Places where the sensor didn't collect data, perhaps due to clouds, are gray.

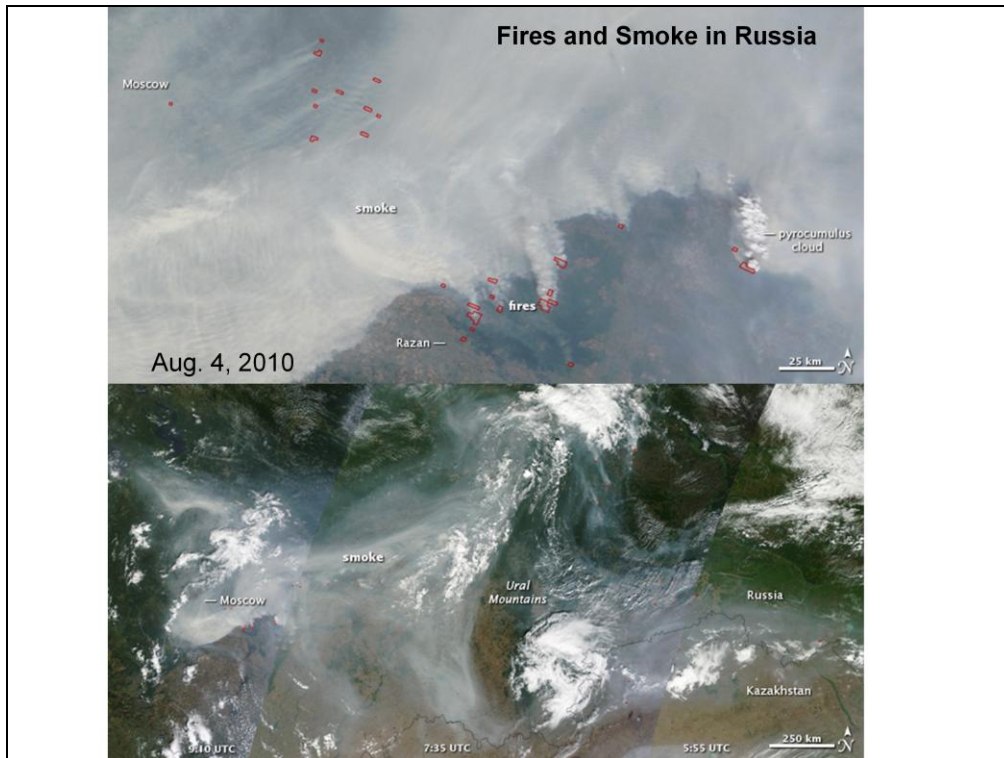
In different parts of the world and in different seasons, the amounts and sources of atmospheric carbon monoxide change. In Africa, for example, the seasonal shifts in carbon monoxide are tied to the widespread agricultural burning that shifts north and south of the equator with the seasons. Fires are an important source of carbon monoxide pollution in other regions of the Southern Hemisphere, such as the Amazon and Southeast Asia.

In the United States, Europe, and eastern China, on the other hand, the highest carbon monoxide concentrations occur around urban areas as a result of vehicle

and industrial emissions. Fires burning over large areas in North America and Russia in some years can be an important source. The MOPITT observations often show that pollution emitted on one continent can travel across oceans to have a big impact on air quality on other continents.

Carbon monoxide is a trace gas in the atmosphere, and it does not have a direct effect on the global temperature, like methane and carbon dioxide do. However, carbon monoxide plays a major role in atmospheric chemistry, and it affects the ability of the atmosphere to cleanse itself of many other polluting gases. In combination with other pollutants and sunshine, it also takes part in the formation of lower-atmospheric (“bad”) ozone and urban smog.

View, download, or analyze more of these data from NASA Earth Observations (NEO): [Carbon Monoxide](#)



Intense fires continued to rage in western Russia on August 4, 2010. Burning in dry peat bogs and forests, the fires produced a dense plume of smoke that reached across hundreds of kilometers. The Moderate Resolution Imaging Spectroradiometer (MODIS) captured this view of the fires and smoke in three consecutive overpasses on NASA's [Terra](#) satellite. The smooth gray-brown smoke hangs over the Russian landscape, completely obscuring the ground in places. The top image provides a close view of the fires immediately southeast of Moscow, while the lower image shows the full extent of the smoke plume.

The fires along the southern edge of the smoke plume near the city of Razan, top image, are among the most intense. Outlined in red, a line of intense fires is generating a wall of smoke. The easternmost fire in the image is extreme enough that it produced a [pyrocumulus cloud](#), a dense towering cloud formed when intense heat from a fire pushes air high into the atmosphere.

The lower image shows the full extent of the smoke plume, spanning about 3,000 kilometers (1,860 miles) from east to west. If the smoke were in the United States, it would extend approximately from San Francisco to Chicago. The MODIS sensor acquired the right section of the image starting at 5:55 UTC (10:55 a.m. local time, 8:55 a.m. in Moscow). The center section is from the overpass starting at 7:35 UTC (11:35 local time, 10:35 in Moscow), and the westernmost section was taken at 9:10 UTC (12:10 p.m. local time in Moscow).

Early analyses of data from the Multi-angle Imaging Spectroradiometer (MISR), another instrument on the Terra satellite, indicates that smoke from previous days has at times reached 12 kilometers (7.5 miles) above Earth's surface into the stratosphere. At such heights, smoke is able to travel long distances to affect air quality far away. This may be one reason that the smoke covers such a large area. The pyrocumulus cloud and the detection of smoke in the stratosphere are good indicators that the fires are large and extremely intense.

According to news reports, 520 fires were burning in western Russia on August 4. MODIS detected far fewer. It is likely that the remaining fires were hidden from the satellite's view by the thick smoke and scattered clouds. [High temperatures](#) and [severe drought](#) dried vegetation throughout central Russia, creating hazardous fire conditions in July.

As of August 4, 48 people had died in the fires and more than 2,000 had lost their homes throughout central Russia, said news reports. The dense smoke also created hazardous air quality over a broad region. Visibility in Moscow dropped to 20 meters (0.01 miles) on August 4, and health officials warned that everyone, including healthy people, needed to take preventative measures such as staying indoors or wearing a mask outdoors, reported the Wall Street Journal. In the image, Moscow is hidden under a pall of smoke. Close to the fires, smoke poses a health risk because it contains small particles (soot) and hazardous gases that can irritate the eyes and respiratory system. Smoke also contains chemicals that lead to ozone production farther away from the fires.

The large image provides the full scene shown in the lower image at the sensor's highest resolution (as shown in the top image). The MODIS Rapid Response Team provides the scene in [additional resolutions](#).

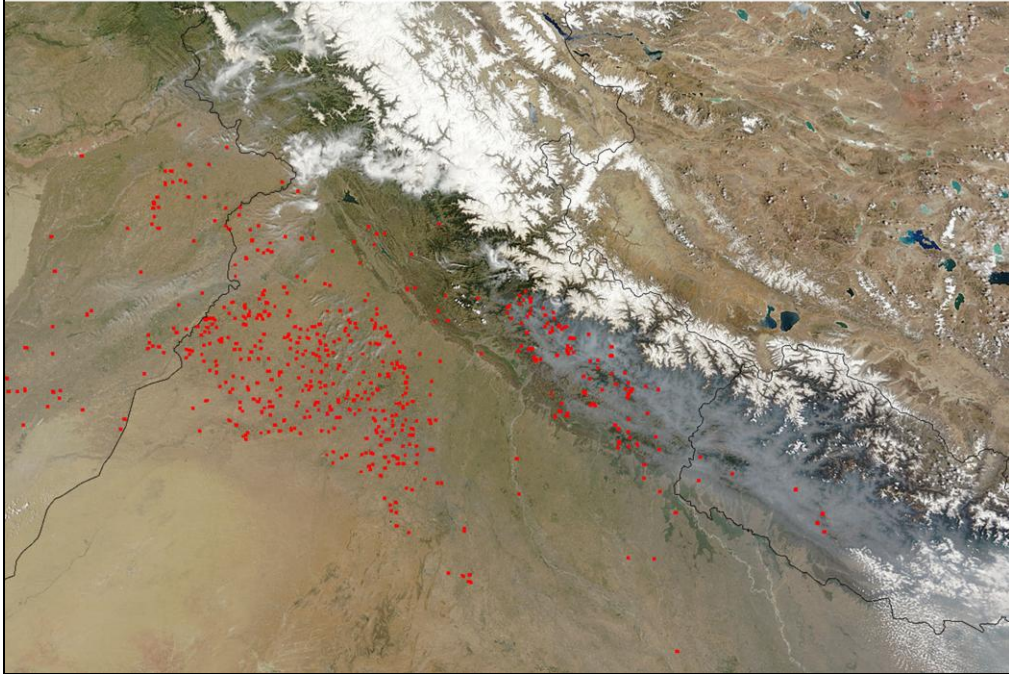
References

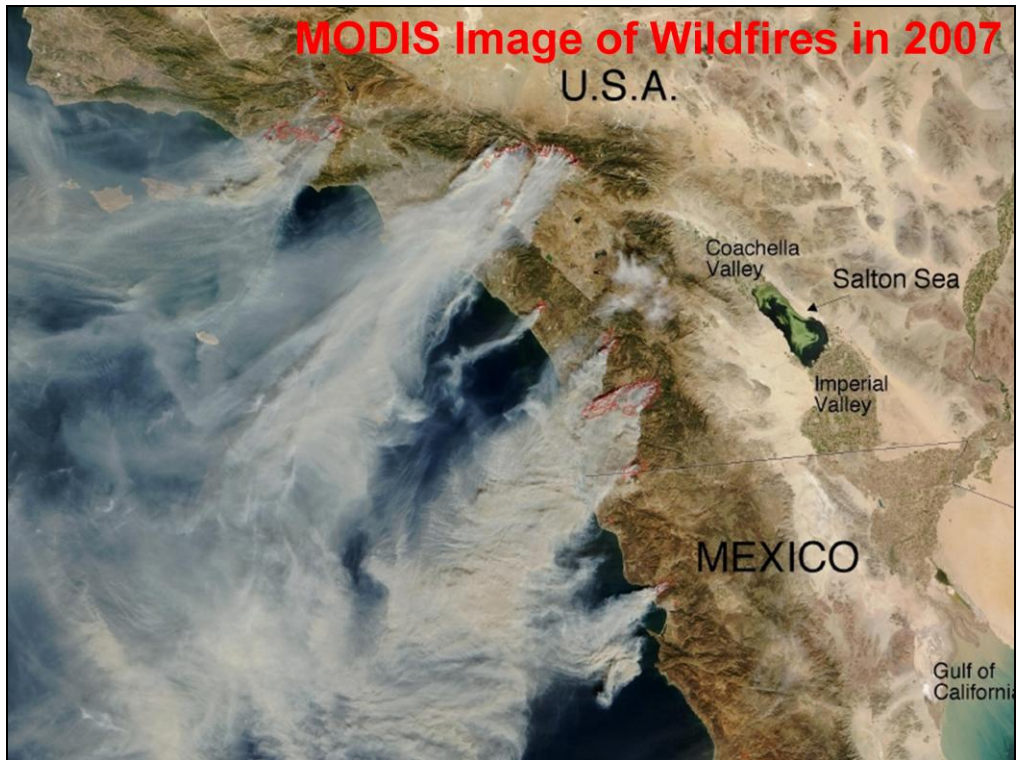
- BBC News. (2010, August 4). [Medvedev cuts holiday as Russian wildfires kill 48](#). Accessed August 4, 2010.
- Iosebashvili, I. (2010, August 4). [Death toll rises as Russian fires rage](#). Wall Street Journal. Accessed August 4, 2010.

[More images of this event in Natural Hazards](#)

NASA image courtesy Jeff Schmaltz, [MODIS Rapid Response Team](#) at NASA GSFC. Caption by Holli Riebeek with information courtesy Mike Fromm, Naval Research Laboratory.

MODIS Rapid Response System 2009/121 - 05/01 at 05 :40 UTC Fires in Northern India Satellite: Terra - Pixel size: 1km





Why use MODIS?

What bands are Showing?

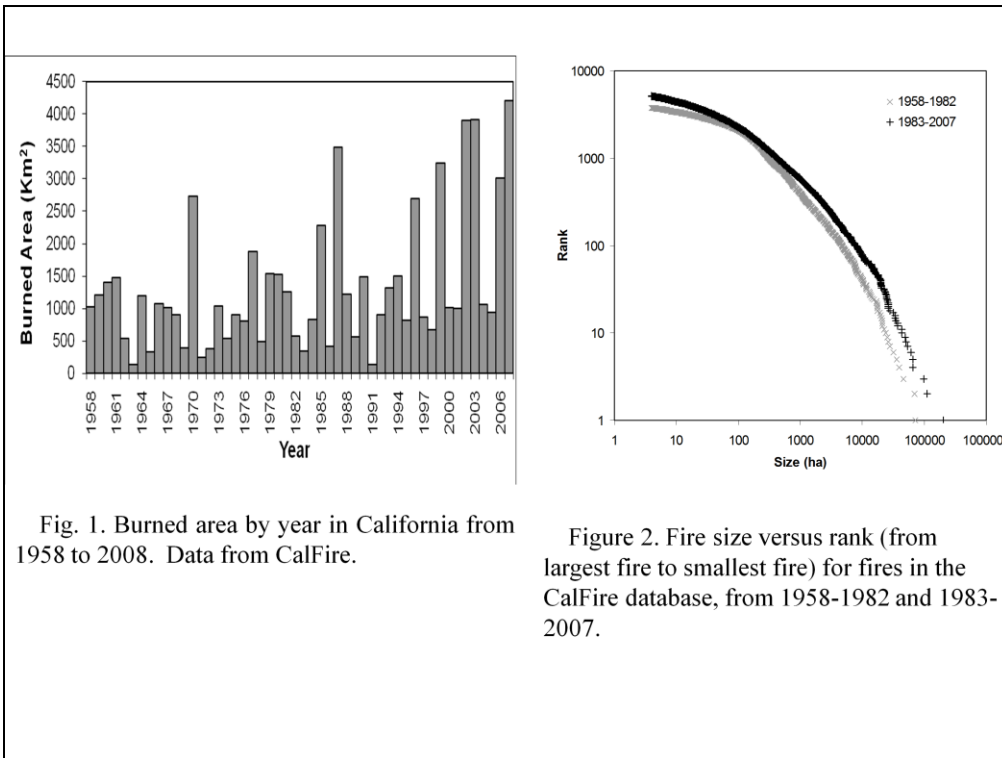
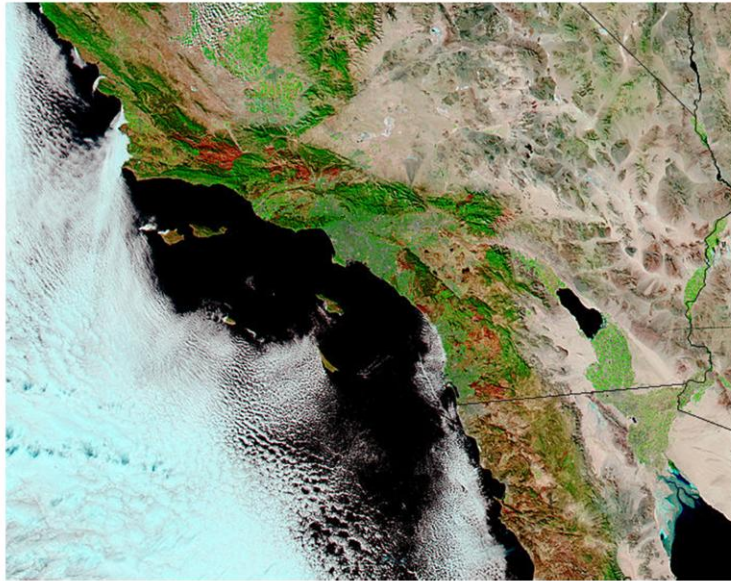


Fig. 1. Burned area by year in California from 1958 to 2008. Data from CalFire.

Figure 2. Fire size versus rank (from largest fire to smallest fire) for fires in the CalFire database, from 1958-1982 and 1983-2007.

MODIS Oct. 31, 2007; burn scars left behind after wildfires devastated the area



On October 31, 2007 NASA's Aqua satellite captured this remarkable image of Southern California, showing the burn scars left behind after wildfires devastated the area.

Satellite: Aqua MODIS - Pixel size: 1km

This image, made using visible and infrared light, shows the extent of the fires over the landscape. The charred areas appear red, unburned vegetation is bright green and bare earth is a tan color.

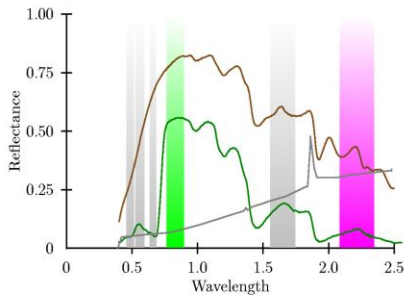
Over the past two weeks the fires have burned more than 500,000 acres, according to the California Department of Forestry and Fire Protection.

Two fires were still burning in Southern California as of November 5, the Santiago and the Poomacha fires. Despite weaker than predicted winds, firefighters were not able to fully contain the blazes over the weekend as they had initially predicted.

The National Weather Service is forecasting little to no wind to affect the area over the upcoming week. Fire officials say they expect full containment of the fires by the end of this coming weekend.

Image credit: NASA MODIS Rapid Response

NORMALIZED BURN RATIO (NBR)



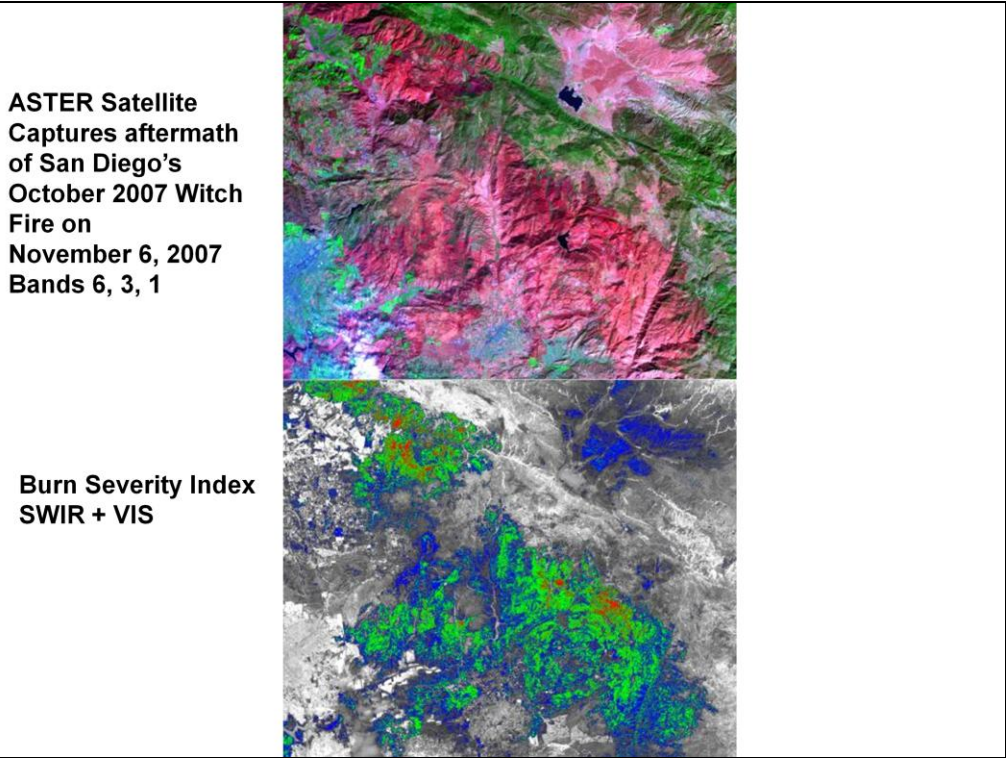
$$(L4 - L7) / (L4 + L7)$$

$$NDBR = NBR_{pre} - NBR_{post}$$

Larger Numbers = burns

[Van Wagtendonk et al., 2004](#) J. Van Wagtendonk, W.R.R. Root and C.H. Key, Comparison of AVIRIS and Landsat ETM+ detection capabilities for burn severity, *Remote Sensing of Environment* **92** (2004), pp. 397–408.

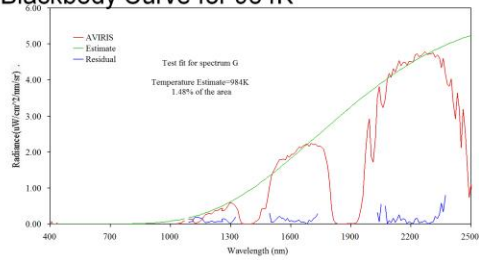
[Key and Benson, 2005](#) C. Key and N.C. Benson, *The Normalized Burn Ratio (NBR): A Landsat TM radiometric measure of burn severity, report, U. S. Geol. Surv., Colo, Boulder* (2005) retrieved from <http://nrmsc.usgs.gov/research/ndbr.htm>.



The extent of San Diego's Witch fire, the most destructive of the recent spate of wildfires in Southern California, is graphically depicted in this November 6 false-color image from the Advanced Spaceborne Thermal Emission and Reflection Radiometer on NASA's Terra spacecraft. Vegetation is shown in green, burned areas in dark red and urban areas in blue (upper image) ASTER Bands 6, 3, and 1. On the burn severity index image (lower image), calculated using infrared and visible bands, red areas are the most severely burned, followed by green and blue.

Size: 37.5 by 45 kilometers (23.1 by 27.8 miles)
Location: 33 degrees North latitude, 116.9 degrees West longitude
Original Data Resolution: ASTER 15 meters (49.2 feet)
Dates Acquired: November 6, 2007

SWIR Reflectance and modeled Blackbody Curve for 984K



Burn Temperature % Area Burned

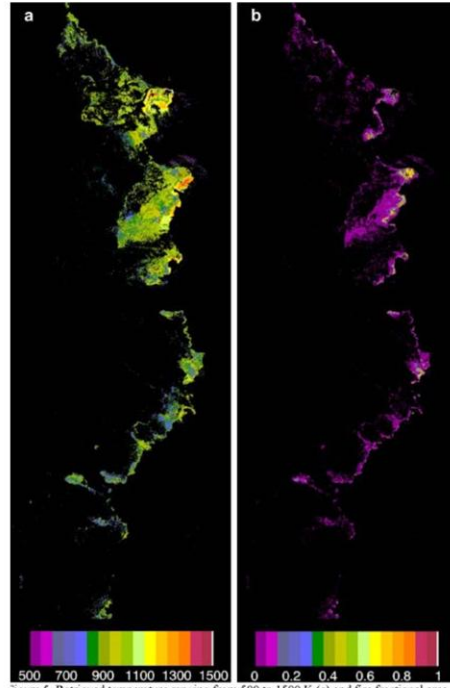
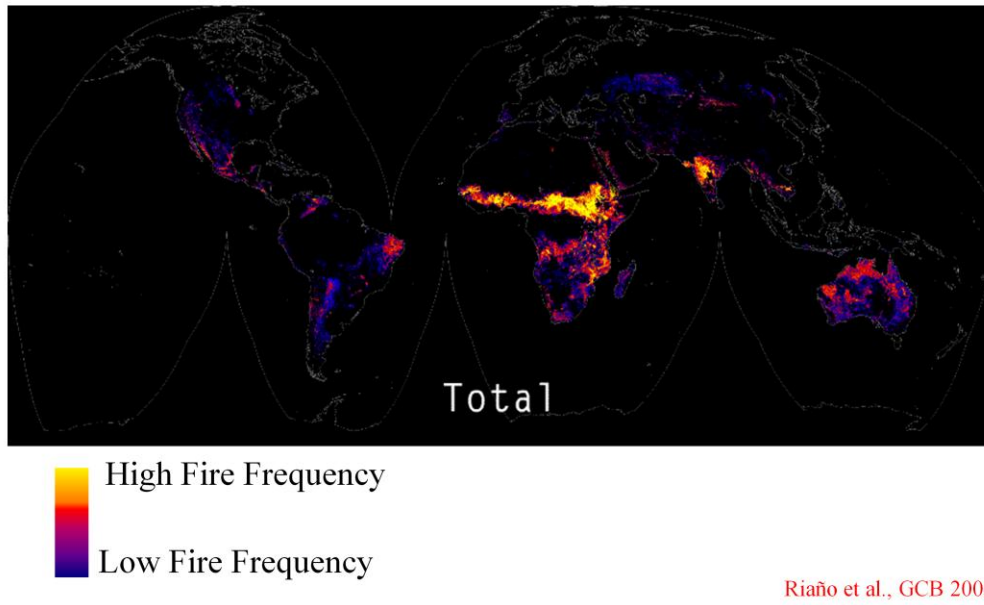


Figure 5. Retrieved temperature ranging from 500 to 1500 K (a) and fire fractional area ranging from 0 to 1 (b).

Global Burned Area Distribution 1981-2000 Using NOAA-NASA Pathfinder



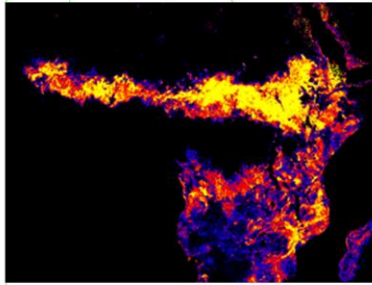
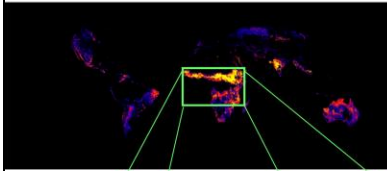
Identify global patterns of burned area at tile level (1000 by 1000 km) with a cluster analysis on the principal components of the time series

Analyze fire frequency and periodicity in the burn cycle

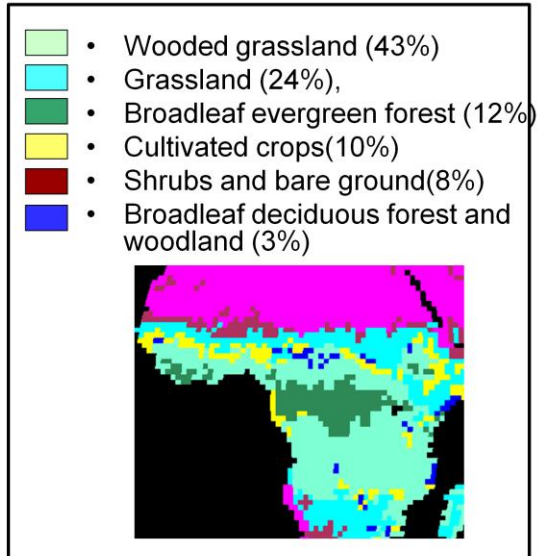
Did burned area increased or decreased for any month or annually over the twenty years at the global scale and for any of the regions identified in the cluster analysis?

Can fire patterns be explained from environmental variables such as land cover, spatial distribution, elevation, and sea influence?

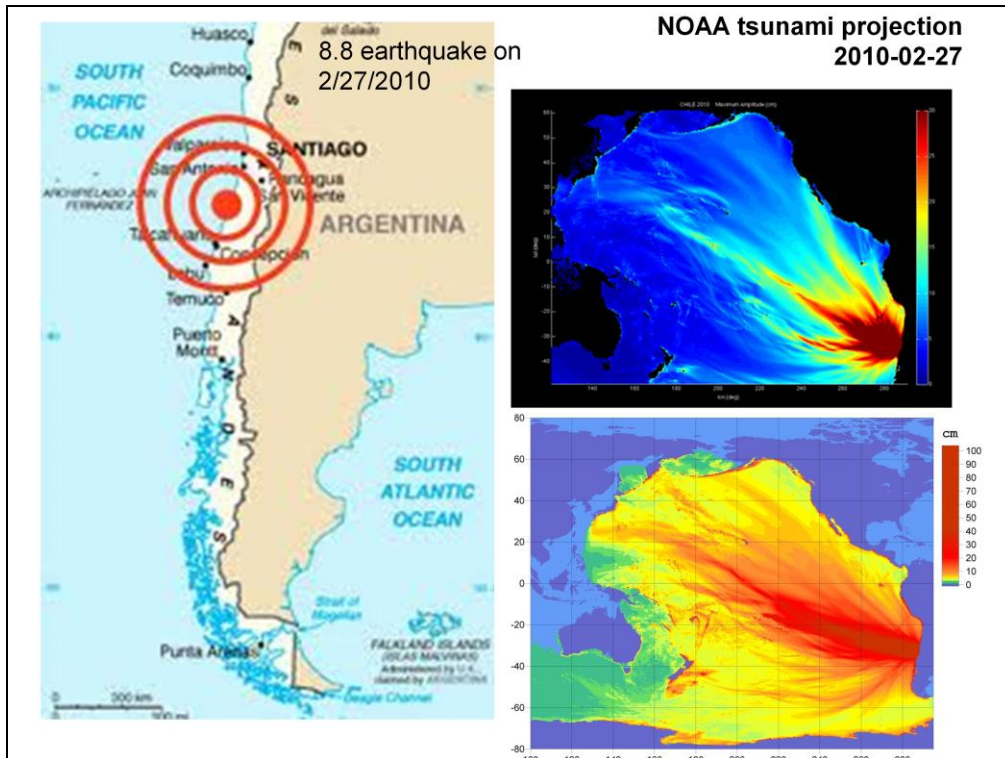
Wildfire Locations In Africa



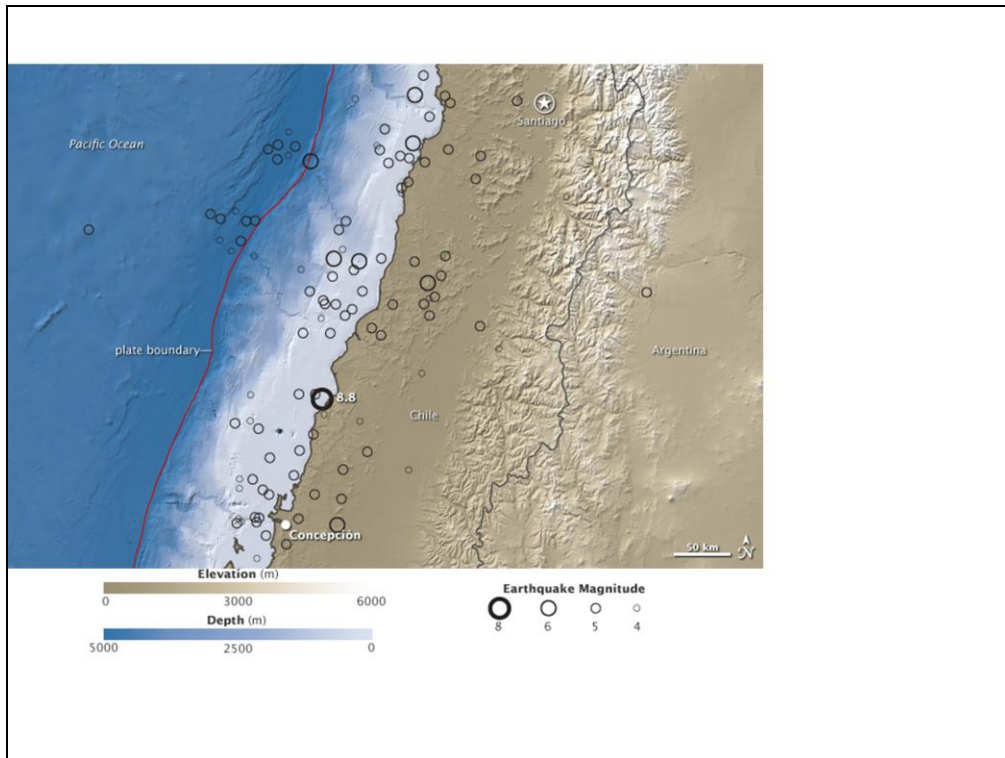
24°N and 20°S latitude

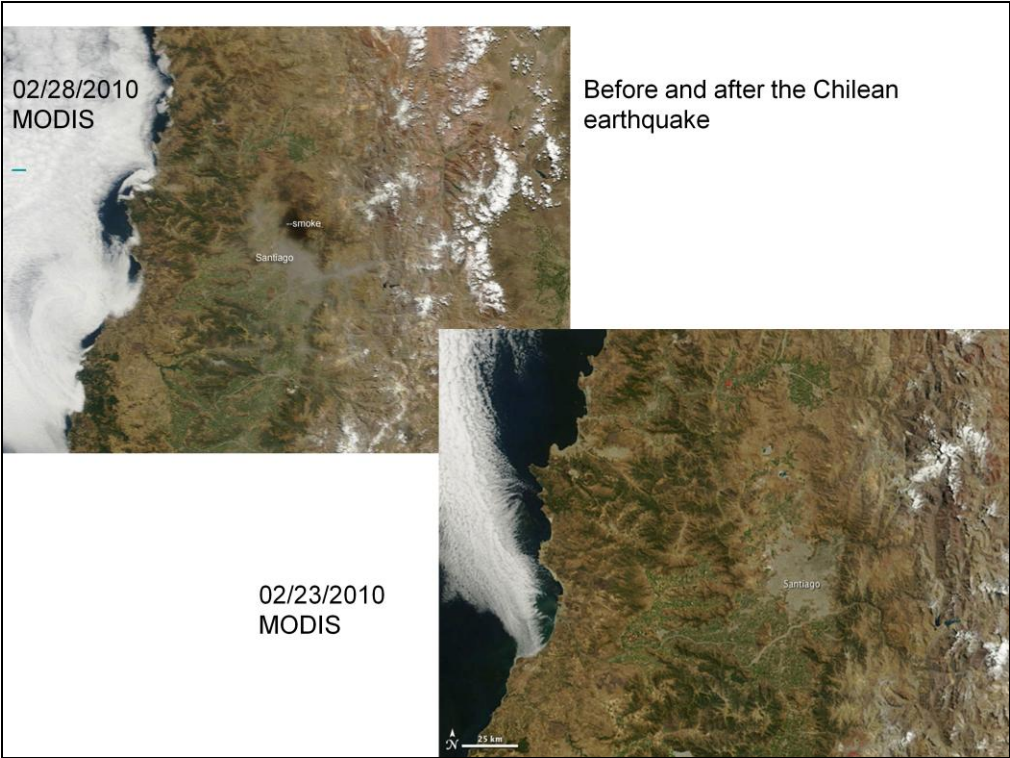


Wooded grassland or savanas

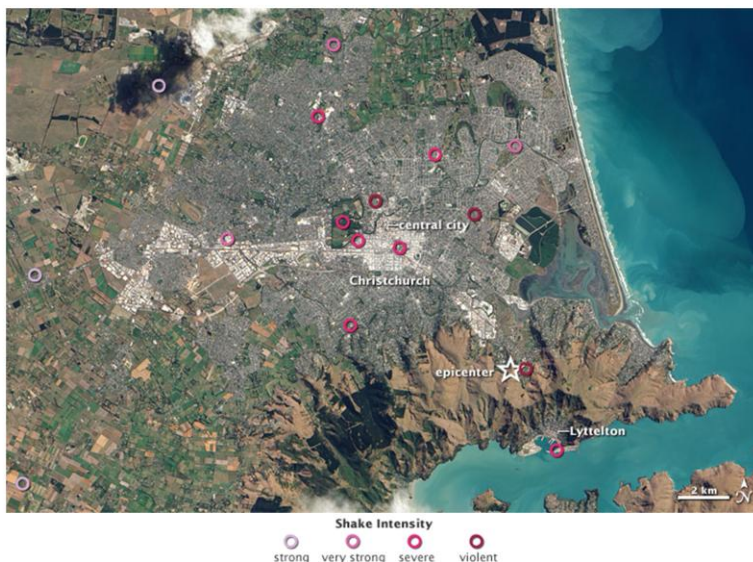


Shortened the earth's rotation by 1.26usecs. Shifted the axis of the earth by 2.7 millimicrosecs.





Christchurch, New Zealand: main 6.3 scale earthquake 22 Feb 2011
Followed a 7.1 earthquake 40km west in Sept. 2010



Natural color, March 1, 2011 ALI on the EO-1

It is a modern human tendency to focus on the number of an earthquake—specifically, the magnitude, or what people used to call the “Richter scale.” But the destruction from a quake usually has more to do with location and timing. Such was the case with the earthquake in Christchurch, New Zealand, on February 22, 2011.

A September 2010 earthquake centered 40 kilometers (25 miles) west of Christchurch, in the plains near Darfield, struck at 4:35 a.m., had a magnitude of 7.1, and caused some structural damage and one death (by heart attack). The earthquake in February 2011 occurred at 12:51 p.m. and just 10 kilometers (6 miles) from the center of Christchurch. It had a magnitude of 6.3, though was officially classified—scientifically speaking—as an aftershock of the 2010 quake. At least 166 people died, and the city of Christchurch was devastated structurally and emotionally. Many people are still missing.

The natural-color image above was captured on March 4, 2011, by the [Advanced Land Imager \(ALI\)](#) on NASA's [Earth Observing-1 \(EO-1\)](#) satellite. Overlain on the map are seismological measurements of the ground shaking in the Christchurch area on February 22, as noted by the U.S. Geological Survey's Earthquake Hazard Program.

The deeper the red color of the circle, the more intense the “peak ground acceleration,” or shaking of the earth. Note how intensity is highest right around the most densely developed areas of Christchurch. City officials and news accounts also described liquefaction—the softening and loosening of the soil due to shaking and groundwater penetration—that was 300 to 500 percent worse than during the September 2010 earthquake.

There are two forms of energy that cause the shaking in an earthquake. “P” or primary waves provide the initial, often vertical, jolt that lifts people and structures off the ground. “S” or secondary waves lead to horizontal shaking. Most structures collapse during the longer-duration S waves because buildings are not designed to handle this side-to-side motion. In Christchurch, the quake occurred so close by that the lag between P and S waves was a mere second.

References

GeoNet (2011, March 4) [Christchurch badly damaged by magnitude 6.3 earthquake](#). Accessed March 8, 2011.

GNS Science (2011, February 25) [February 22nd earthquake in Christchurch](#). Accessed March 8, 2011.

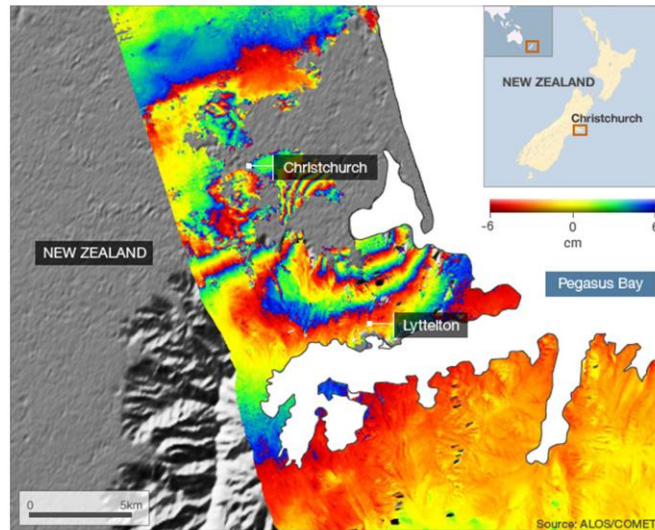
New Zealand Herald (2011, February) [Christchurch earthquake: Levels of liquefaction 300-500 pc worse](#). Accessed March 8, 2011.

U.S. Geological Survey (n.d.) [Shake Map: South Island of New Zealand](#). Accessed March 8, 2011.

NASA Earth Observatory image by Robert Simmon, using ALI data from the [EO-1](#) Team and USGS [Earthquake Hazard Program](#). Caption by Mike Carlowicz.

Instrument: EO-1 - ALI

22 February 2010 earthquake in Christchurch, NZ, is illustrated in interferometry radar imagery.



The coloured bands, or fringes, represent movement towards or away from the spacecraft

The upheaval wrought by the 22 February earthquake in Christchurch, NZ, is illustrated in new radar imagery.

The Magnitude 6.3 tremor killed more than 160 people and shattered a city already reeling from a previous seismic event in September.

Data from the [Japanese Alos spacecraft](#) has been used to map the way the ground deformed during the most recent quake.

It shows clearly that the focus of the tremor was right under the city's south-eastern suburbs.

The type of image displayed on this page is known as a synthetic aperture radar interferogram.

John Elliott Oxford University

It is made by combining a sequence of radar images acquired by an orbiting satellite "before" and "after" a quake.

The technique allows very precise measurements to be made of any ground motion that takes place between the image acquisitions.

The coloured bands, or fringes, represent movement towards or away from the spacecraft.

In this interferogram, the peak ground motion is almost 50cm of motion towards the satellite.

"It's like a contour map but it's showing to the south-east of Christchurch that the ground motion is towards Alos. That's uplift," explained Dr John Elliott from the Centre for the Observation and Modelling of Earthquakes and Tectonics ([Comet](#)) at Oxford University, UK.

"And then right under Christchurch, we see subsidence. That's partly due to liquefaction but it's mainly due to the way the Earth deforms when you snap it like an elastic band."

Where the rainbow fringes become most tightly spaced is where the fault break came closest to the surface, although the data indicates the fault is unlikely to have broken right through to the surface.

Blind danger Liquefaction is a phenomenon that afflicts loose sediments in an earthquake and is akin to a lateral landslide.

It is a major issue for Christchurch because the city is built on an alluvial plain, and this type of ground will amplify any shaking during a tremor.

BBC News reader Gillian Needham took this image of central Christchurch moments after the quake struck New Zealand's second city on 22 February

Scientists are using the Alos information to understand better the future seismic hazards in this part of New Zealand.

It has become obvious from recent events that Christchurch sits close to "blind" faulting - faulting that is at risk of rupture, but which betrays little evidence of its existence at the surface, meaning the potential danger it poses is not fully recognised.

"It means much more work needs to be done around Christchurch," said Dr Elliot.

"People knew they could get earthquakes further into the mountains [in the west of South Island]; that's how they've been built in some ways, through earthquakes and all the faulting.

"But to get an earthquake right under their city will have been a surprise to nearly every single person."

Liquid lurch The interferogram is noticeably incomplete - there are several areas where the fringing is missing. There are a number of reasons for this.

To the east is ocean, and this technique does not work over water.

To the west, the issue is related to the satellite track and the fact that it views the Earth in strips. Hence, you get bands of data.

But the more interesting and more relevant omissions are in Christchurch itself.

Dr Elliot commented: "Here, the patches are the result of de-correlation between the acquisition images, where we just can't match them - they're too different.

"There are a few reasons for that. Usually it's the result of vegetation growth, but here it could be due to more extreme shaking or liquefaction."

Tuesday's quake was less energetic but more destructive

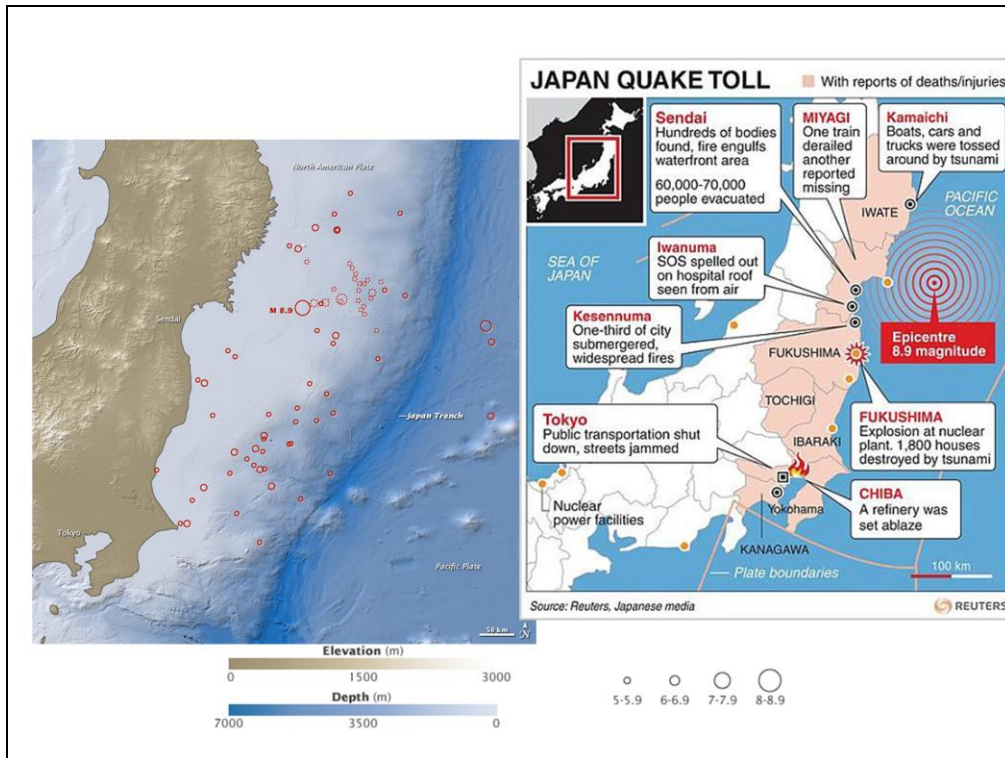
Researchers are investigating the relationship between September's Magnitude 7.1 quake and last month's 6.3 event.

The latter is very much considered to be an aftershock from the former, even though they were separated by six months.

The September quake occurred about 40km to the west, rupturing a similar length of fault. The most recent tremor ruptured about 15km of fault.

What scientists need to know now is the nature of any "seismic gap" between the two; that is, a segment of fault which was not broken in either tremor but which may have been loaded with additional strain because of both those events.

The Advanced Land Observing Satellite (Alos) was launched in 2006



On March 11, 2011, at 2:46 p.m. local time (05:46 Universal Time, or UTC), a magnitude 8.9 earthquake struck off the east coast of Japan, at 38.3 degrees North latitude and 142.4 degrees East longitude. The epicenter was 130 kilometers (80 miles) east of Sendai, and 373 kilometers (231 miles) northeast of Tokyo. If initial measurements are confirmed, it will be the world's [fifth largest earthquake since 1900](#) and the worst in Japan's history.

This map shows the location of the March 11 earthquake, as well as the foreshocks (dotted lines) and aftershocks (solid lines). The size of each circle represents the magnitude of the associated quake or shock. The map also includes land elevation data from NASA's [Shuttle Radar Topography Mission](#) and ocean bathymetry data from the British Oceanographic Data Center.

According to the U.S. Geological Survey (USGS), the earthquake occurred at a depth of 24.4 kilometers (15.2 miles) beneath the seafloor. The March 11 earthquake was preceded by a series of large foreshocks on March 9, including an M7.2 event. USGS reported that the earthquakes "occurred as a result of [thrust faulting](#) on or near the [subduction zone](#) interface plate boundary."

The March 11 quake sent tsunami waves rushing into the coast of Japan and rippling out across the entire Pacific basin. Crescent-shaped coasts and harbors, such as those near Sendai, can play a role in focusing the waves as they approach the shore. Also, since land elevation is low and flat along much of the Japanese coast, many areas are particularly vulnerable to tsunamis.

The [Japan Meteorological Agency reported](#) maximum tsunami heights of 4.1 meters at Kamaishi at 3:21 p.m. (06:21 UTC), 7.3 meters at 3:50 p.m. (06:50 UTC) at Soma, and 4.2 meters at 4:52 p.m. (07:52 UTC) at Oarai.

The U.S. Pacific Tsunami Warning Center (PTWC) reported a wave with maximum height of 2.79 meters (9.2 feet) at an observing station at Hanasaki, Hokkaido, at 3:57 p.m. local time (06:57 UTC). Other PTWC reports:

- 1.27 meters (4.2 feet) at 10:48 UTC at Midway Island
- 1.74 meters (5.7 feet) at 13:72 UTC at Kahului, Maui, Hawaii
- 1.41 meters (4.6 feet) at 14:09 UTC at Hilo, Hawaii
- 0.69 meters (2.3 feet) at 15:42 UTC in Vanuatu
- 1.88 meters (6.2 feet) at 16:54 UTC at Port San Luis, California
- 2.02 meters (6.6 feet) at 16:57 UTC at Crescent City, California

References

- Japan Meteorological Agency (2011, March 11). [Latest Tsunami Information](#). Accessed March 11, 2011.
- Pacific Tsunami Warning Center (2011, March 11). [Tsunami Messages for the Pacific Ocean](#). Accessed March 11, 2011.
- U.S. Geological Survey (2011, March 11). [Magnitude 8.9 - Near The East Coast of Honshu, Japan](#). Accessed

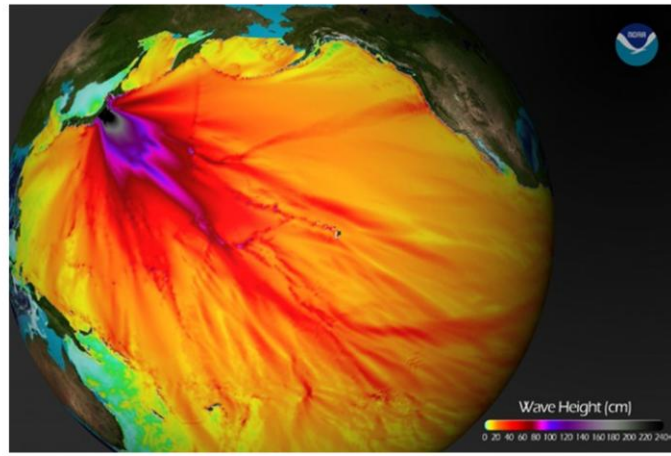
March 11, 2011.



The German Aerospace Centre captured these dramatic photographs of Soma. The one on the left was taken on September 5, 2010, and the one on the right was taken yesterday after the devastating tsunami

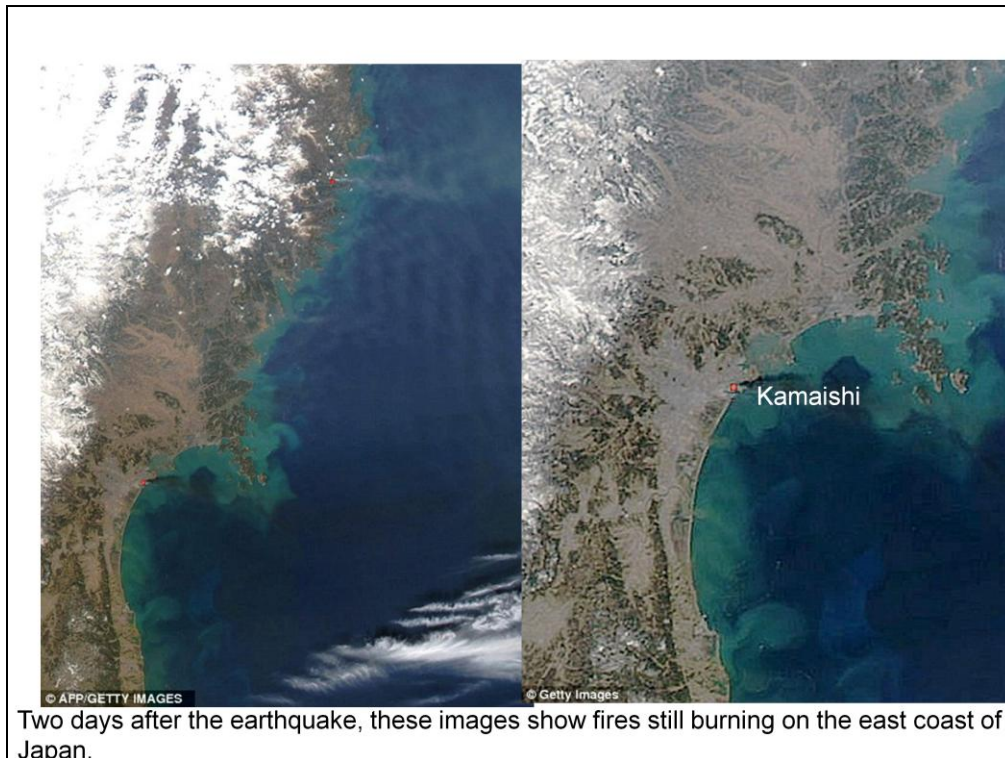
Read more: <http://www.dailymail.co.uk/news/article-1365882/Japan-earthquake-Tsunami-satellite-pictures->

Simulation of Tsunami wave





This photo combo shows an area of Yuriage near the Miyagi Prefecture, Japan, on April 4, 2010, left, and March 12, 2011. Geoeye data



Two days after the earthquake, these images show fires still burning on the east coast of Japan. The image on the left shows Kamaishi (top red dot) and Sendai towards the bottom. The image on the right is a close-up of Sendai where acrid smoke pours over the sea

Read more: <http://www.dailymail.co.uk/news/article-1365882/Japan-earthquake-Tsunami-satellite-pictures-devastation.html#ixzz1GYHnpBAe>

Two days after the earthquake, these images show fires still burning on the east coast of Japan. The image on the left shows Kamaishi (top red dot) and Sendai towards the bottom. The image on the right is a close-up of Sendai where acrid smoke pours over the sea

Read more: <http://www.dailymail.co.uk/news/article-1365882/Japan-earthquake-Tsunami-satellite-pictures-devastation.html#ixzz1GYHnpBAe>



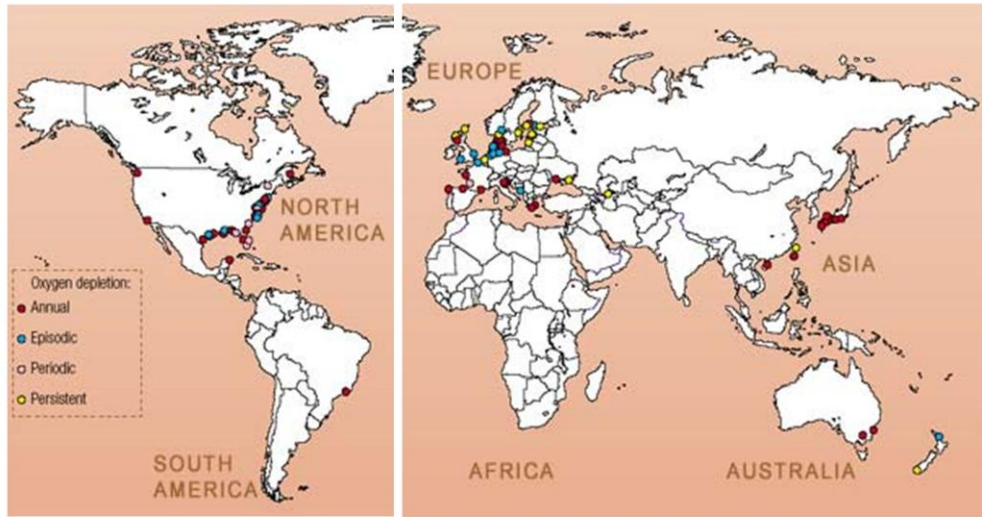
Still combination images of Natori taken by Geo Eye 1 Satellite on April 4, 2010 and March 12, 2011.



The pictures, compiled by Google, Nasa, German Aerospace Centre and Taiwan's National Space Organisation reveal how far inland the wall of water travelled and the trail of destruction that it left behind.

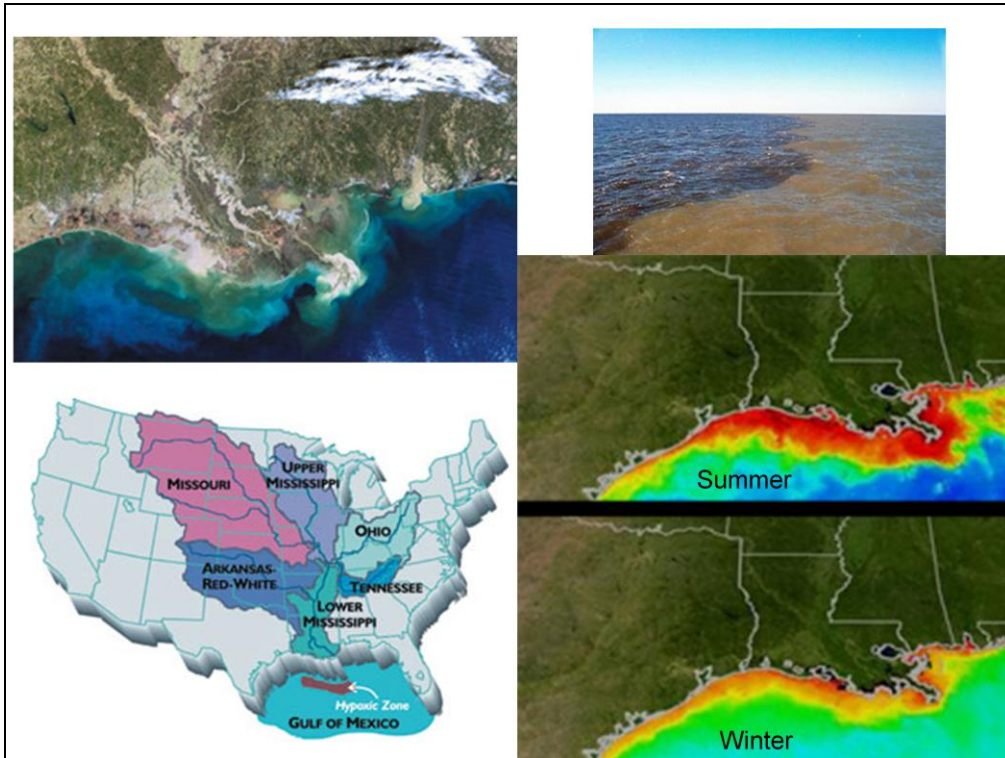
Read more: <http://www.dailymail.co.uk/news/article-1365882/Japan-earthquake-Tsunami-satellite-pictures-devastation.html#ixzz1GYHJ4WMB>

Coastal Dead Zones Around the World



Source:

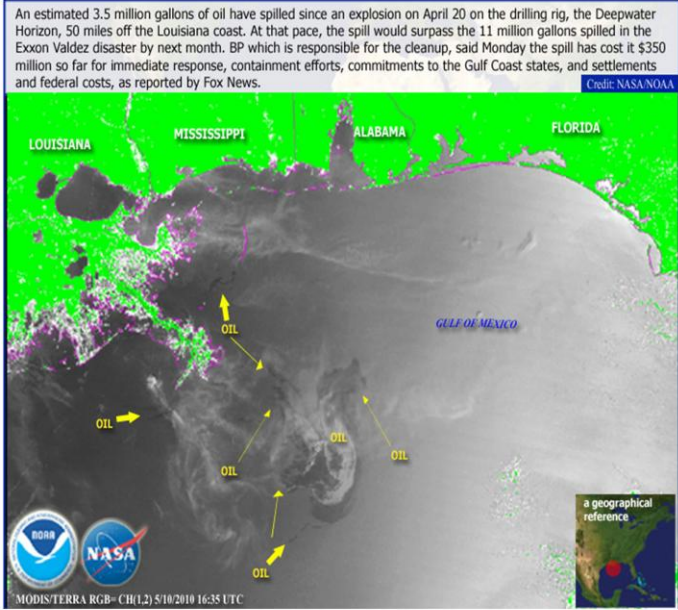
UNEP, GEO Yearbook 2003 (Nairobi: 2004), compiled from Boesch 2002, Caddy 2000, Diaz et al. (in press), Green and Short 2003, Rabalais 2002



This satellite image of summer conditions in the Gulf of Mexico south of Texas, Louisiana and Mississippi (US) is from the MODIS/Aqua satellite. Red and orange colors indicate the large amounts of phytoplankton that have multiplied because of nitrogen-rich water entering the Gulf at the Mississippi River Delta. When the phytoplankton die and decompose, oxygen is taken from the water and other marine life can not survive. This is known as a dead zone.

NASA - MODIS/Aqua

NOAA Significant Event Imagery for May 10, 2010





June 19, 2010

On Saturday, June 19, 2010, oil spread northeast from the leaking Deepwater Horizon well in the Gulf of Mexico. The oil appears as a maze of silvery-gray ribbons in this photo-like image from the Moderate Resolution Imaging Spectroradiometer ([MODIS](#)) on NASA's [Aqua](#) satellite.

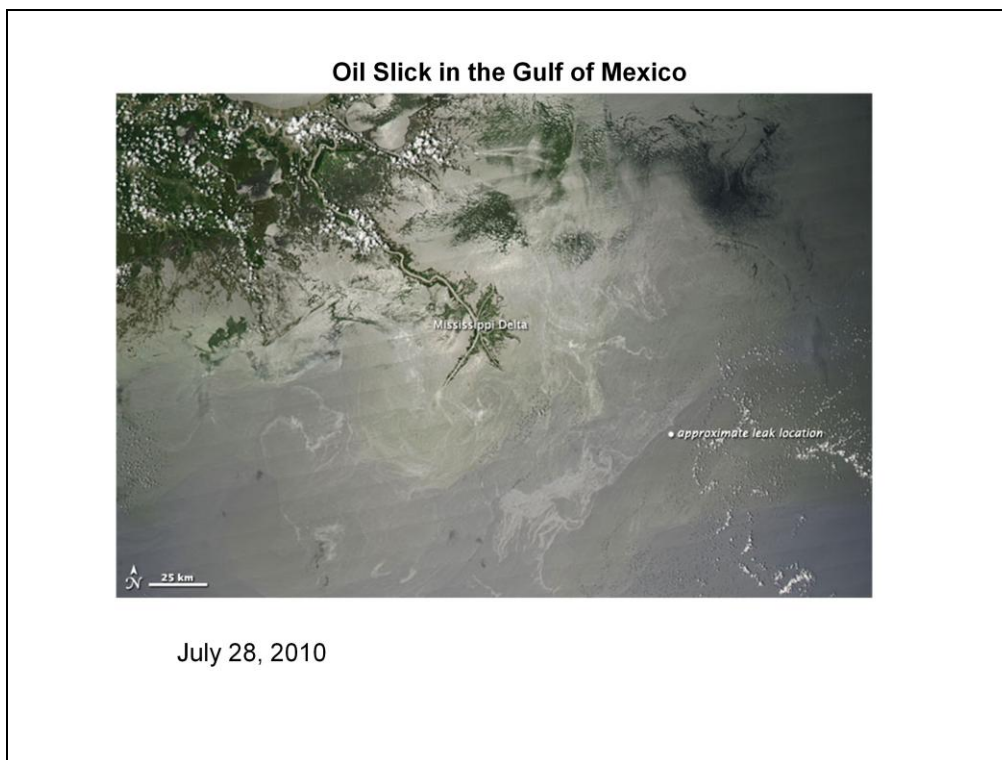
The location of the leaking well is marked with a white dot. North of the well, a spot of black may be smoke; reports from the National Oceanic and Atmospheric Administration say that oil and gas continue to be captured and burned as part of the emergency response efforts.

The large image provided above is at MODIS' maximum spatial resolution (level of detail). Twice-daily images of the [Gulf of Mexico](#) are available from the MODIS Rapid Response Team in additional resolutions and formats, including a georeferenced version that can be used in Google Earth.

References

National Oceanic and Atmospheric Administration. (2010, June 20). [Deepwater Horizon Incident, Gulf of Mexico](#). National Ocean Service, Office of Response and Restoration. Retrieved June 21, 2010.

[More images of this event in Natural Hazards](#)



On July 24, 2010, the administrator of the U.S. National Oceanic and Atmospheric Administration (NOAA), Jane Lubchenco, provided a [briefing](#) about the anticipated impact of [Tropical Storm Bonnie](#) on the Deepwater Horizon oil slick in the Gulf of Mexico. Bonnie was expected to help dissipate and weather the oil on the sea surface, spreading out the slick, lowering surface concentrations, and making the oil more amenable to biodegradation. On July 28, 2010, after Bonnie had passed through the region, NOAA reported less oil observed on Gulf of Mexico overflights.

The Moderate Resolution Imaging Spectroradiometer ([MODIS](#)) on NASA's [Aqua](#) satellite captured this natural-color image on July 28, 2010. Around the location of the oil leak, and around the Mississippi Delta, relatively light swirls and patches appear on the ocean surface. These areas might be oil slicks, although other factors could affect the water's ability to reflect sunlight, especially near the shore. If these pale-hued sheens are oil-slicked areas, they contain very little recoverable oil, according to NOAA.

In the months since the Deepwater Horizon accident, the Earth Observatory has been able to show oil slicks in the Gulf of Mexico only under certain conditions, namely clear skies and sunlight hitting the water at an appropriate angle. To learn more about our oil slick images, including why the oil isn't visible every day, please visit [Gulf of Mexico Oil Slick Images: Frequently Asked Questions](#).

Related Resources

[RestoreTheGulf.gov](#) is the official federal portal for the Deepwater BP oil spill response and recovery.

[Current information about the extent of the oil slick](#) is available from the Office of Response and Restoration at the National Oceanic and Atmosphere Administration.

[Information about the impact of the oil slick on wildlife](#) is provided by the U.S. Fish and Wildlife Service.

[More images of this event in Natural Hazards](#)

NASA image by Jeff Schmaltz, [MODIS Rapid Response Team](#). Caption by Michon Scott.

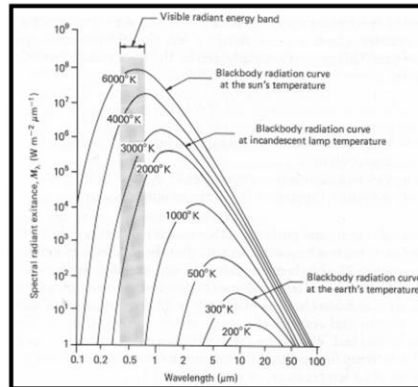
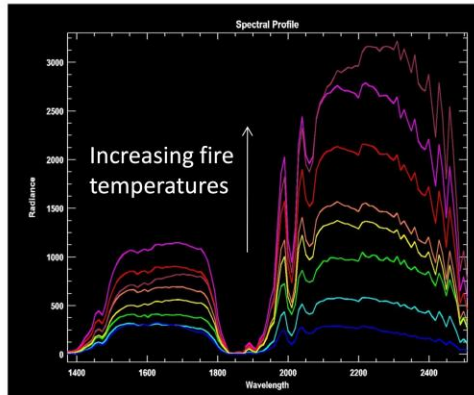
Instrument: Aqua - MODIS

What you should know from today's lecture:

1. Be able to identify different types of natural disasters suitable for monitoring
2. What types of remote sensing data are used and why
3. Analysis ranges from visual interpretation to more complex analyses? Why
4. Rapid processing and release of remote sensing data for public safety
5. Monitoring recovery

Mapping fire temperatures

Both quantity of radiance emitted and the wavelength of peak emission vary with T, making it possible to estimate fire temperature.



Planck's Law (derived from $E = hv = hc/\lambda$)
Energy is transferred from a warm body to a colder body

$$I'(\lambda, T) = \frac{2hc^2}{\lambda^5} \frac{1}{e^{\frac{hc}{\lambda kT}} - 1}$$



Max Planck

$I(\lambda, T)$ = Intensity = energy per unit surface area per unit time per unit solid angle as a function of wavelength

h = Planck's constant (6.626×10^{-34} J s)

c = speed light

k = Boltzmann's constant

The spectral radiance of EM radiation at all wavelengths from a black body at temperature T .

As a function of wavelength λ , Planck's law written (for unit solid angle) as:

This function peaks for $hc = 4.97\lambda kT$, a factor of 1.76 shorter in wavelength (higher in frequency) than the frequency peak (can be calculated as frequency instead of wavelength).

I' is the spectral radiance or energy per unit time per unit surface area per unit solid angle per unit wavelength (or frequency)

Stefan-Boltzmann Law (for ideal blackbodies)

M_b is derived from Planck's equation as $M_{b,\lambda} = \sigma T^4$

Total radiated energy (j or watts/m²) by a black-body = $(\sigma) * T^4$

$$\sigma = 5.6697 \times 10^{-8} \text{ W m}^{-2} \text{ K}^{-4} \mu\text{m K}$$

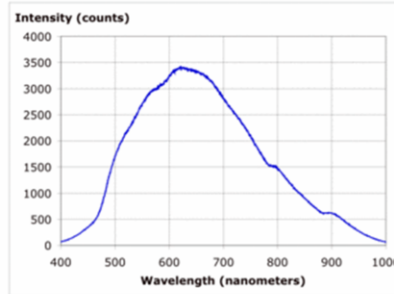


Josef Stefan



Ludwid Boltzmann

The Sun produces more spectral radiant exitance (M_b) at 6,000 K than the Earth at 300 K. As the temperature increases, the total amount of radiant energy measured in watts per m² (the area under the curve) increases and the radiant energy peak shifts to shorter wavelengths.



The spectrum of an incandescent bulb in a typical flashlight. Here, the filament temperature appears to be about 4600 K due to a peak emittance around 630 nm. The shape shows that the filament is not a true black body.

For Gray Bodies S-B Expressed As:

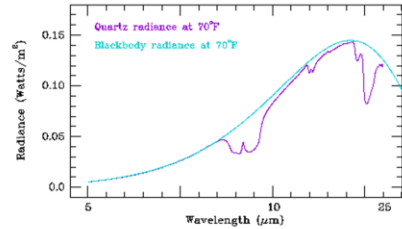
Incorporating **Emissivity (ϵ) allows calculation of
Radiant flux of non-blackbody materials**

$$M_{\lambda} = \epsilon \sigma T^4$$

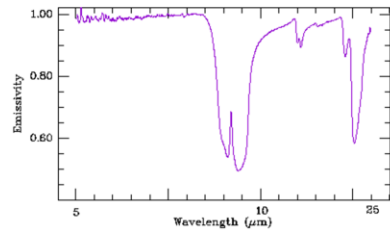
Emissivity

Emissivity (ϵ) is the ratio between the true radiant flux from an object (M_r) and the blackbody emission at the same temperature (M_b).

$$\epsilon_\lambda = M_r/M_b = (T_{\text{rad}}/T_{\text{kin}})^4$$



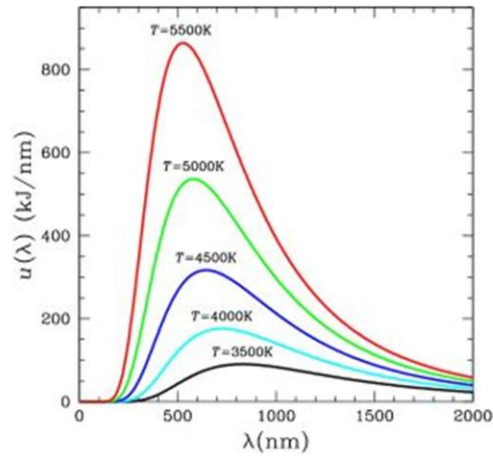
Quartz radiance spectrum along with a blackbody radiance spectrum at the same temperature.



Quartz emissivity spectrum: the result of dividing quartz radiance by blackbody radiance at the same temperature.

Emissivity can be estimated by measuring both the radiant temperature and the kinetic temperature at the same time.

Relationship between Temperature and Wavelength: Wein's Displacement Law



Wilhelm Wien



Wein's Displacement Law

The relationship between the true temperature of a blackbody (T) in degrees Kelvin and its peak spectral exitance or dominant wavelength (λ_{max}) is described by Wein's displacement law:

$$\lambda_{max} = \frac{k}{T} \approx \frac{2898 \mu\text{m K}}{T}$$

where k is a constant equaling $2898 \mu\text{m } ^\circ\text{K}$

Equal signs should be approximately equal≈